
MUBen: Benchmarking the Uncertainty of Pre-Trained Models for Molecular Property Prediction

Yinghao Li¹, Lingkai Kong¹, Yuanqi Du², Yue Yu¹, Yuchen Zhuang¹, Wenhao Mu¹,
Chao Zhang¹

¹Georgia Institute of Technology, Atlanta, GA 30332 ²Cornell University, Ithaca, NY 14850
¹{yinghao.li, lkkong, yueyu, yc Zhuang, wmu30, chaozhang}@gatech.edu
²yd392@cornell.edu

Abstract

Large Transformer models pre-trained on massive unlabeled molecular data have shown great success in predicting molecular properties. However, these models can be prone to overfitting during fine-tuning, resulting in over-confident predictions on test data that fall outside of the training distribution. To address this issue, uncertainty quantification (UQ) methods can be used to improve the models' calibration of predictions. Although many UQ approaches exist, not all of them lead to improved performance. While some studies have used UQ to improve molecular pre-trained models, the process of selecting suitable backbone and UQ methods for reliable molecular uncertainty estimation remains underexplored. To address this gap, we present MUBen, which evaluates different combinations of backbone and UQ models to quantify their performance for both property prediction and uncertainty estimation. By fine-tuning various backbone molecular representation models using different molecular descriptors as inputs with UQ methods from different categories, we critically assess the influence of architectural decisions and training strategies. Our study offers insights for selecting UQ and backbone models, which can facilitate research on uncertainty-critical applications in fields such as materials science and drug discovery.

1 Introduction

The task of molecular representation learning is pivotal in scientific domains and bears the potential to facilitate research in fields such as chemistry, biology, and materials science [77]. Nonetheless, supervised training typically requires vast quantities of data, which may be challenging to acquire due to the need for expensive laboratory experiments [15]. With the advent of self-learning Transformers [76] pioneered by BERT [13] and GPT [63], there has been a surge of interest in creating large-scale pre-trained molecular representation models from readily available and inexpensive *unlabeled* molecular data [78, 87, 64, 48, 90, 72]. Such large pre-trained backbone models have demonstrated impressive representational capabilities, achieving state-of-the-art performance on a variety of molecular property prediction tasks [84].

However, in many molecular applications, there is a pressing need for reliable predictions that are not only precise but also *uncertainty-aware*. The provision of calibrated uncertainty estimates allows us to distinguish “noisy” predictions and thus improve model robustness [22], or estimate data distributions, which can enhance downstream tasks such as active learning [19], high throughput screening [52, 58], or wet-lab experimental design [15, 89, 69, 12, 39]. Unfortunately, large-scale models [27, 43] can easily overfit the fine-tuning data and exhibit misplaced confidence in their predictions. Several works have investigated and developed various uncertainty quantification (UQ) methods on molecular property prediction tasks [34, 52, 8, 69, 12, 26] and in neighboring research

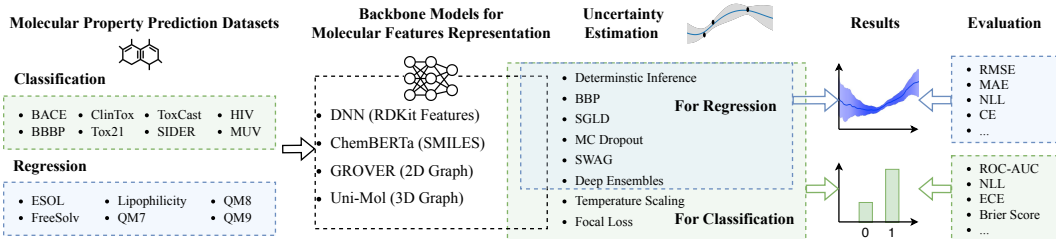


Figure 1: An overview of MUBen with all datasets, backbone models, UQ methods, and metrics enumerated. Elements in green and blue are related to classification and regression tasks, respectively.

areas such as protein engineering [25]. For instance, Bust et al. [8] have extended a message passing neural network (MPNN) [23] with post-hoc recalibration [27] to address the overconfidence issue in molecular property prediction. Soleimany et al. [69] have applied evidential message passing networks [68, 2] to quantitative structure-activity relationship regression tasks. Deshwal et al. [12] have utilized Bayesian optimization to conduct reliable predictions of Nanoporous material properties and to direct experiments.

Despite their contributions, these studies exhibit several limitations: **1)** the variety of uncertainty estimation methods considered is limited, and some effective strategies might be unintentionally overlooked; **2)** their prediction focus is confined to a limited range of molecular property prediction scenarios, *e.g.*, only quantum mechanics prediction, failing to explore a broader spectrum of tasks; and **3)** none of these studies embrace the power of recent large-scale pre-trained models, which have shown remarkable performance in various downstream tasks. To the best of our knowledge, a comprehensive evaluation of UQ methods applied to these pre-trained molecular representation models is currently lacking and warrants further investigation.

We present MUBen, a benchmark specifically designed to assess UQ performance applied to the pre-trained molecular representation models for both molecular property classification and regression tasks. An overview of MUBen is presented in Figure 1. It encompasses UQ methods from various categories, including deterministic prediction, Bayesian neural networks, post-hoc calibration, and ensembles (§ 4.2), all backbone by a set of molecular representation models, each of which uniquely relies on a molecular descriptor from a distinct perspective (§ 4.1). MUBen delivers intriguing results and insights that may guide the selection of backbone model and/or UQ methods in practice (§ 5). We structure our code, available at <https://github.com/Yinghao-Li/UncertaintyBenchmark>, to be user-friendly, easily transferrable, and extendable, with the hope that this work will promote the future development of UQ methods, pre-trained models, or applications within the domains of materials science and drug discovery.

2 Related Works

Pre-Trained Molecular Representation Models Existing pre-trained models for molecular representation learning can be distinguished into three categories, based on the type of molecular descriptors they utilize as input. The first category includes models like ChemBERTa [10], SMILES-BERT [78], and Molformer [65], which leverage string-based descriptors such as SMILES for molecular representation. During the pre-training stage, these models predict randomly masked tokens in a similar fashion to BERT [13]. Given that molecules can be represented as 2D topological graphs, with atoms serving as nodes and bonds as edges, a second category of pre-training strategies has emerged. These models employ techniques such as context prediction [32, 64], contrastive learning [74, 87, 79], and replaced component detection [46, 38] to learn molecular representation with the awareness of the graph context. Recently, the research community has also started to explore pre-training methods using 3D geometric graphs as a third category [16, 48, 90, 72]. For example, GEM [16] incorporates bond angles and bond lengths as additional edge attributes to enrich the 3D information. Similarly, Uni-Mol [90] employs a 3D position recovery loss and a masked atom prediction loss to effectively learn 3D spatial representations of molecules.

Uncertainty Quantification Uncertainty estimation plays a crucial role in enabling deep neural networks to acknowledge what they don’t know, which have been applied to various domains including object detection [9, 28], natural language processing [36, 88, 54], time series forecasting [61, 37, 75] and decision making [3, 42]. Uncertainty estimation for neural networks can be categorized in two directions. The first line is called Bayesian neural networks (BNNs) which quantify predictive uncertainty by imposing probability distributions over model parameters instead of using point estimates. While BNNs provide a principled way of uncertainty quantification, exact inference of parameter posteriors is often intractable. Existing works adopt Monte Carlo dropout [18], variational inference [6, 40] and Markov chain Monte Carlo (MCMC) [82] for approximate inference.

Along another line, several non-Bayesian methods have also been proposed. Deep ensembles [45, 17] estimates uncertainty by training multiple networks with different initializations. Temperature scaling [60, 27] learns a single parameter to rescale all the logits for better calibration on a held-out validation set and is extended to regression tasks [70]. Evidential network [68, 2, 69] treats the predictions as subjective opinions and learns the function that collects the evidence leading to these opinions by a deterministic neural net from data. Recently, conformal prediction [4, 5] is proposed to produce sets that are guaranteed to contain the ground truth with a user-specified probability.

UQ methods have also been applied to molecular property estimation [69, 12, 39, 33] and reaction prediction [67] for obtaining a calibrated predictive models. Although [66, 31] also attempt to compare different UQ methods for molecules, they only focus on a small set of tasks (no more than 4 datasets), as well as non-pretrained models. Instead, we cover a diverse suite of tasks in MUBen with multiple strong pre-trained molecular property prediction models, which can serve as a standard benchmark to faithfully evaluate the ability of UQ approaches.

3 Problem Setup

Let \mathbf{x} denote a descriptor of a molecule, such as SMILES or a 2D topological graph. We define y as the label with domain $y \in \{1, \dots, K\}$ for K -class classification or $y \in \mathbb{R}$ for regression. θ denotes all parameters of the molecular feature extractor and the task-specific layer. We assume that a training dataset \mathcal{D} consists of N i.i.d. samples $\mathcal{D} = \{(\mathbf{x}_n, y_n)\}_{n=1}^N$. Our goal is to fine-tune the parameters θ using the training dataset and learn a calibrated predictive probability model $p_\theta(y|\mathbf{x}_n)$. The quality of the uncertainty estimates can be evaluated using the following metrics.

Negative Log-Likelihood Negative log-likelihood (NLL) is often utilized to assess the quality of model uncertainty on holdout sets. Despite being a proper scoring rule as per Gneiting’s framework [24], it does have certain limitations. For instance, NLL tends to overemphasize tail probabilities, as outlined by Quinero Candela et al. [62].

Brier Score Brier score (BS) [7] is a proper scoring rule for measuring the accuracy of predicted probabilities. It is computed as the mean squared error of a predicted probability vector, $p_\theta(y|\mathbf{x}_n)$, and the categorical ground-truth label y_n : $BS = \frac{1}{K} \sum_y (p_\theta(y|\mathbf{x}_n) - \mathbf{1}(y = y_n))^2$, where $\mathbf{1}$ is the indicator function. The Brier score provides an insightful decomposition as $BS = \text{Uncertainty} - \text{Resolution} + \text{Reliability}$ [56]. “Uncertainty” corresponds to the inherent variability over labels; “Resolution” quantifies the deviation of individual predictions from the average; and “Reliability” gauges the extent to which predicted probabilities align with the actual probabilities.

Expected Calibration Error Expected calibration error (ECE) [57] measures the correspondence between predicted probabilities and empirical accuracies for classification tasks. It first divides the predicted probabilities $\{p_\theta(y_n | \mathbf{x}_n)\}_{n=1}^N$ into S bins $B_s = \{n \in \{1, \dots, N\} | p_\theta(y_n | \mathbf{x}_n) \in (\rho_s, \rho_{s+1}]\}$ with $s \in \{1, \dots, S\}$ and then compute the weighted average gap between the accuracy and predicted probabilities within each bin. That is, $ECE = \sum_{s=1}^S \frac{|B_s|}{N} |\text{acc}(B_s) - \text{conf}(B_s)|$, where $\text{acc}(B_s) = \frac{1}{|B_s|} \sum_{n \in B_s} \mathbf{1}(y_n = \hat{y}_n)$, $\text{conf}(B_s) = \frac{1}{|B_s|} \sum_{n \in B_s} p_\theta(\hat{y}_n | \mathbf{x}_n)$, and $\hat{y}_n = \arg \max_y p_\theta(y | \mathbf{x}_n)$ is the n -th prediction.

Regression Calibration Error Regression calibration error (CE) [44] is defined similarly to ECE but for regression calibration evaluations. It calculates the true frequency of the predicted points lying in each confidence interval against the predicted fraction of points in that interval. Specifically,

$CE = \frac{1}{S} \sum_{s=1}^S (\frac{s}{S} - |\{n \in \{1, \dots, N\} | F_{\theta}(y_n | \mathbf{x}_n) \leq \frac{s}{S}\}|/N)^2$, where $\frac{s}{S}$ is the expected quantile and $F_{\theta}(y_n | \mathbf{x}_n)$ represents the predicted quantile value of y_n . For example, for Gaussian predictions, $F_{\theta}(\cdot | \mathbf{x}_n) = \Phi(\cdot; \hat{y}_n, \hat{\sigma}_n)$ is the Gaussian CDF parameterized by the predicted mean \hat{y}_n and variance $\hat{\sigma}_n$. We provide more illustrations about this metric in appendix D.

4 Experiment Setup

4.1 Backbone Models

To examine how different molecular descriptor inputs affect model performance across various datasets, we evaluate three widely-adopted backbone models, each of which accepts a unique molecular descriptor as input. Molecular descriptors such as fingerprints, SMILES strings, and 2D or 3D graphs [85], package the structural data of a molecule from varying viewpoints into a format that computational algorithms can readily process. When paired with distinct model architectures carrying divergent inductive biases, these descriptors can offer varied benefits depending on the specific task.

We select various pre-trained Transformer encoders [76, 13] as our backbone models, which include: **1) ChemBERTa** [10, 1], which accepts SMILES strings as input; **2) GROVER** [64], pre-trained with 2D molecular graphs via a Transformer bolstered by a dynamic message-passing graph neural network; and **3) Uni-Mol** [90], which incorporates 3D molecular conformations into its input, and pre-trains specialized Transformer architectures to encode the invariant spatial positions of atoms and represent the edges between atom pairs. In addition, we implement a straightforward **4)** fully connected deep neural network (**DNN**) that uses 200-dimensional RDKit features as input, serving as a comparison baseline. This simple model aims to highlight the performance difference between manual heuristic feature generators and their larger, more complex counterparts that draw upon self-supervised learning processes for knowledge acquisition. For more detailed information, please refer to appendix B.

4.2 Uncertainty Quantification Methods

In MUBen, we choose popular UQ methods from different categories. We provide a high-level sketch here of each method and leave the detailed description to appendix C.

Deterministic Uncertainty Prediction In standard practice, deep classification networks utilize SoftMax or Sigmoid outputs to distribute prediction weights among target classes. Such weights serve as an estimate of the model’s uncertainty. In regression tasks, rather than one single output value, models often parameterize an independent Gaussian distribution with predicted means and variances for a data point, and the variance magnitude acts as an estimate of the model’s uncertainty. We refer to this method as “**deterministic**” in the following discussion.

An alternate loss function for classification is the **Focal loss** [47, 55], which minimizes a regularised KL divergence between the predicted values and the true labels. The regularization increases the entropy of the predicted distribution while the KL divergence is minimized, mitigating the model overconfidence and improving the uncertainty representation.

Bayesian Learning and Inference BNNs estimate the probability distribution over the parameters of the network. Specifically, BNNs operate on the assumption that the weights of each network layer follow a predefined distribution, often a multivariate Gaussian. This distribution’s posterior is maximized by optimizing the model with the feature-label pairs present in the training dataset. During the inference phase, multiple network instances can be sampled by randomly drawing network parameters from the weight distributions. Each instance then independently makes predictions for the input data points, and the prediction distribution inherently captures the desired uncertainty information. Some notable methods that employ this approach include:

- **Bayes by Backprop (BBP)** [6, 40] first introduced Monte Carlo gradients, an extension of the Gaussian reparameterization trick [41], to learn the posterior distribution of network weights directly through backpropagation.
- **Stochastic Gradient Langevin Dynamics (SGLD)** [82] applies Langevin dynamics to infuse noise into the stochastic gradient descent training process, thereby mitigating the overfitting of

network parameters. The samples generated via Langevin dynamics can be used to form Monte Carlo estimates of posterior expectations during the inference stage.

- **Monte Carlo Dropout (MC Dropout)** [18] demonstrates that applying dropout is equivalent to a Bayesian approximation of the probabilistic deep Gaussian process (GP) [11]. Uncertainty is derived from an ensemble of results from multiple stochastic forward passes with dropout enabled.
- **Stochastic Weight Averaging Gaussian (SWAG)** [51] provides an efficient way of estimating Gaussian posteriors over network weights by utilizing stochastic weight averaging (SWA) [35] combined with low-rank & diagonal Gaussian covariance approximations.

Post-Hoc Calibration A Deterministic classification model often outputs over- or under-confident values that are diverged from the model’s true confidence to its prediction. Post-hoc calibration is proposed to address this mismatch, of which the most popular ones are **Platt scaling** [60] and **temperature scaling** [30, 27]. They multiply the output logits before the Sigmoid or SoftMax activation to a scaling factor, which is trained through supervised training on a held-out calibration set to optimize. Experiment shows that temperature scaling improves the calibration in general [27].

Deep Ensembles The ensemble method has long been used in machine learning to improve model performance [14] but was first adopted to estimate uncertainty in [45]. It trains a deterministic network multiple times with different random seeds and combines their predictions at inference. Although simple, it is effective as the ensembles can explore training modes thoroughly in the function space and thus is robust to noisy and out-of-distribution examples, yielding accurate uncertainty estimation.

4.3 Datasets

We carry out our experiments on MoleculeNet [84], a comprehensive collection of widely-utilized datasets for predicting molecular properties. These datasets encompass a broad array of molecular properties, including quantum mechanics, hydration free energy, solubility, and toxicity. Our benchmark incorporates both classification datasets (BACE, BBBP, ClinTox, Tox21, ToxCast, SIDER, HIV, and MUV) and regression datasets (ESOL, FreeSolv, Lipophilicity, QM7, QM8, and QM9). A dataset may contain one or multiple tasks. All classification labels are binary.

In line with previous studies [16, 90], we divide all datasets using scaffold splitting with an 8:1:1 training-validation-test ratio. This approach differs slightly from the random splitting strategy proposed by MoleculeNet for some datasets. However, it minimizes the impact of dataset randomness and, consequently, enhances the reliability of the evaluation. Moreover, scaffold splitting ensures that the scaffolds in each dataset partition are as distinct as possible, inherently causing the validation/test features to fall outside the distribution of the training set. This property is advantageous for our uncertainty evaluations. For detailed descriptions of each dataset, please check appendix A.

4.4 Evaluation Metrics and Protocols

Consistent with recommendations in [84] and previous works [16, 90], we report ROC-AUC (area under the receiver operating characteristic curve) as the metric for classification performance and RMSE (root-mean-square error) and MAE (mean absolute error) for regression tasks. In quantifying classification uncertainty, we use ECE, NLL, and Brier Score as introduced in § 3. For regression, we compute the Gaussian negative log-likelihood, also marked as NLL, which parameterizes a Gaussian distribution with predicted mean and variance and then calculates the likelihood of the actual label: $-\frac{1}{N} \sum_{n=1}^N \log \mathcal{N}(y_n; \hat{y}_n, \hat{\sigma}_n)$, where $\hat{y}_n \in \mathbb{R}$ is the predicted mean $\hat{\sigma}_n \in \mathbb{R}_+$ the variance.

For classification experiments, the output logits are converted to class probabilities using the Sigmoid function, and models are trained with the binary cross-entropy loss unless a specific UQ method necessitates a different approach. Under this configuration, we actually utilize Platt scaling without the bias term as the post-hoc classification calibration. However, due to the prevalence of the term, we refer to it as temperature scaling. We follow [27] and optimize the temperature on the validation dataset. For regression, we standardize each dataset’s training labels by mapping them to a standard Gaussian distribution. Models are trained with standardized labels, and the predicted test values are converted back to the original distribution according to the label mean and variance from the training set before metrics are computed. For datasets with multiple prediction tasks, each classification model features a unique final output head for *each* task, while regression models are equipped with two—

Table 1: Summary of classification results. The first two primary result columns, Tox21 and ToxCast, present metric scores on these example datasets which serve as representative examples, highlighting the trends observable across all datasets. The third primary column, average ranking, provides the rank of each model’s UQ metrics against all other backbone-UQ combinations averaged from all classification datasets. The symbol \uparrow denotes that a higher metric value implies superior performance, while \downarrow denotes the reverse. Text in bold signifies the top-performing uncertainty quantification method within each individual backbone model, and cells in blue indicate the best performance across all backbone-UQ combinations. “ROC” represents ROC-AUC.

	Tox21				ToxCast				Average Ranking			
	ROC \uparrow	ECE \downarrow	NLL \downarrow	BS \downarrow	ROC \uparrow	ECE \downarrow	NLL \downarrow	BS \downarrow	ROC \downarrow	ECE \downarrow	NLL \downarrow	BS \downarrow
DNN-RDKit												
Deterministic	0.7386	0.0417	0.2771	0.0779	0.6222	0.1168	0.4436	0.1397	25.75	17.25	24.13	22.88
Temperature	0.7386	0.0342	0.2723	0.0773	0.6220	0.1114	0.4882	0.1398	25.75	15.38	21.25	19.88
Focal Loss	0.7374	0.1058	0.3161	0.0871	0.6289	0.1264	0.4389	0.1396	25.88	24.38	22.38	24.00
MC Dropout	0.7376	0.0356	0.2727	0.0763	0.6248	0.1093	0.4319	0.1358	26.50	13.00	19.38	18.63
SWAG	0.7364	0.0438	0.2793	0.0790	0.6207	0.1175	0.4441	0.1400	26.38	18.50	25.63	23.50
BBP	0.7243	0.0422	0.2847	0.0814	0.6020	0.1443	0.4673	0.1510	22.75	19.13	19.38	21.38
SGLD	0.7257	0.1192	0.3455	0.0978	0.5319	0.3054	0.6685	0.2378	27.75	26.00	28.88	27.88
Ensembles	0.7540	0.0344	0.2648	0.0746	0.6486	0.0900	0.4008	0.1292	20.00	7.13	11.75	13.13
ChemBERTa												
Deterministic	0.7542	0.0571	0.2962	0.0812	0.6554	0.1209	0.4313	0.1330	15.63	17.38	18.88	19.38
Temperature	0.7542	0.0424	0.2744	0.0792	0.6540	0.1067	0.4817	0.1313	15.88	12.00	13.88	15.38
Focal Loss	0.7523	0.0969	0.3052	0.0845	0.6442	0.1197	0.4243	0.1346	17.63	20.13	17.88	20.63
MC Dropout	0.7641	0.0423	0.2697	0.0744	0.6624	0.1069	0.4070	0.1276	12.50	10.75	10.63	10.00
SWAG	0.7538	0.0592	0.3008	0.0818	0.6556	0.1202	0.4305	0.1327	16.13	19.50	21.38	20.38
BBP	0.7433	0.0459	0.2765	0.0780	0.5814	0.1276	0.4545	0.1469	20.88	19.00	16.00	19.50
SGLD	0.7475	0.0504	0.2784	0.0795	0.5436	0.2238	0.5602	0.1881	21.13	19.88	19.13	18.63
Ensembles	0.7681	0.0440	0.2679	0.0750	0.6733	0.1037	0.3986	0.1258	12.38	13.00	11.63	12.25
GROVER												
Deterministic	0.7808	0.0358	0.2473	0.0694	0.6587	0.1043	0.4091	0.1298	11.63	11.50	8.88	9.88
Temperature	0.7810	0.0291	0.2439	0.0686	0.6496	0.1424	0.4612	0.1424	12.63	8.88	7.50	9.25
Focal Loss	0.7779	0.1148	0.3052	0.0811	0.6359	0.1221	0.4365	0.1383	15.00	23.38	21.50	22.25
MC Dropout	0.7817	0.0346	0.2455	0.0689	0.6615	0.1009	0.4042	0.1288	11.25	10.50	7.63	8.63
SWAG	0.7837	0.0360	0.2482	0.0689	0.6603	0.1060	0.4114	0.1301	9.13	11.63	8.88	8.38
BBP	0.7697	0.0438	0.2552	0.0711	0.5995	0.1731	0.5090	0.1660	16.75	22.00	14.75	15.88
SGLD	0.7635	0.0402	0.2558	0.0716	0.5542	0.2712	0.6194	0.2139	18.75	18.63	15.25	15.63
Ensembles	0.7876	0.0316	0.2411	0.0675	0.6646	0.1034	0.4061	0.1290	8.50	8.13	5.38	6.88
Uni-Mol												
Deterministic	0.7895	0.0454	0.2601	0.0716	0.6734	0.1020	0.3983	0.1274	11.50	15.50	16.13	13.88
Temperature	0.7896	0.0346	0.2483	0.0704	0.7028	0.1456	0.4566	0.1355	11.00	12.00	13.13	12.75
Focal Loss	0.7904	0.0972	0.2899	0.0785	0.6934	0.1227	0.4079	0.1284	10.00	23.50	19.38	20.50
MC Dropout	0.7891	0.0480	0.2628	0.0726	0.6833	0.1074	0.4015	0.1274	12.88	19.88	19.25	17.25
SWAG	0.7842	0.0593	0.2994	0.0728	0.6870	0.1085	0.4005	0.1271	10.13	22.13	22.25	18.25
BBP	0.7932	0.0396	0.2520	0.0703	0.6273	0.1296	0.4522	0.1456	12.13	17.00	15.50	16.25
SGLD	0.7887	0.0433	0.2569	0.0684	0.5700	0.1953	0.5207	0.1717	14.75	18.13	18.88	14.50
Ensembles	0.8052	0.0332	0.2389	0.0662	0.6841	0.0953	0.3877	0.1247	5.13	8.88	7.63	6.50

for predicting the mean \hat{y} and another for the variance $\hat{\sigma}$, which is guaranteed to be positive using a SoftPlus function [45]. Regression models are trained with Gaussian NLL objective. We apply validation-based early stopping for parameter selection on all experiments unless the UQ method has other requirements.

We compute the metrics for each task individually before calculating their macro average. Each reported metric is the average of 3 individual training-test runs with random seeds 0, 1, and 2. This differs from deep ensembles, which aggregate model predictions *prior* to metric calculation. The number of ensembled models for deep ensembles is 3 for larger datasets including MUV, QM8, and QM9, and 10 for other smaller ones (the dataset statistics are presented in Table 3). For Bayesian methods that require sampling during inference, we aggregate the results from 30 test runs for each trained model before calculating the metrics.

5 Results and Analysis

Tables 1 and 2 present the primary prediction and uncertainty quantification scores for classification and regression, respectively, derived from two representative datasets. These tables also provide the macro-averaged rankings of each method across all datasets referenced in § 4.3. Further insights can be gained from Figure 2, which visualizes the Mean Reciprocal Ranks (MRRs) for each backbone

Table 2: Summary of regression test results including metric scores for two example datasets—ToxCast and QM9, and the averaged model ranks.

	Lipophilicity				QM9				Average Ranking			
	RMSE↓	MAE↓	NLL↓	CE↓	RMSE↓	MAE↓	NLL↓	CE↓	RMSE↓	MAE↓	NLL↓	CE↓
DNN-RDKit												
Deterministic	0.7575	0.5793	0.6154	0.0293	0.01511	0.01012	-3.379	0.04419	16.67	15.67	11.33	10.50
MC Dropout	0.7559	0.5773	0.9071	0.0341	0.01480	0.01000	-3.526	0.04327	15.17	15.17	11.33	10.67
SWAG	0.7572	0.5823	0.7191	0.0308	0.01524	0.01019	-3.284	0.04495	18.00	17.67	14.00	12.50
BBP	0.7730	0.5938	0.7578	0.0305	0.01534	0.01025	-3.347	0.04452	21.17	20.50	10.33	7.33
SGLD	0.7468	0.5743	0.2152	0.0090	0.01958	0.01437	-3.335	0.00702	19.83	19.33	6.83	1.83
Ensembles	0.7172	0.5490	0.6165	0.0322	0.01430	0.00956	-3.602	0.04362	11.50	11.17	6.33	8.67
ChemBERTa												
Deterministic	0.7553	0.5910	1.2368	0.0362	0.01464	0.00916	-2.410	0.05468	17.83	16.67	18.83	14.67
MC Dropout	0.7142	0.5601	0.8178	0.0349	0.01412	0.00880	-3.150	0.05133	14.33	13.83	15.00	13.67
SWAG	0.7672	0.5992	1.5809	0.0395	0.01477	0.00925	-2.170	0.05535	19.33	18.50	20.33	15.83
BBP	0.7542	0.5869	0.4419	0.0279	0.01443	0.00928	-2.593	0.05399	17.67	18.50	10.83	9.00
SGLD	0.7622	0.5982	0.8719	0.0355	0.01530	0.01012	-3.758	0.03378	19.83	20.50	9.50	8.50
Ensembles	0.7367	0.5763	0.9756	0.0360	0.01397	0.00868	-2.876	0.05425	14.83	13.83	14.67	12.67
GROVER												
Deterministic	0.6316	0.4747	2.1512	0.0478	0.01148	0.00678	-0.787	0.06206	10.67	11.67	17.67	16.00
MC Dropout	0.6293	0.4740	2.0526	0.0476	0.01140	0.00676	-1.100	0.06161	9.33	11.17	16.00	14.33
SWAG	0.6317	0.4750	2.3980	0.0485	0.01156	0.00678	-0.477	0.06252	12.33	13.33	20.33	17.83
BBP	0.6481	0.5058	0.0789	0.0196	0.01179	0.00700	-1.885	0.05909	14.17	15.67	7.67	4.00
SGLD	0.6360	0.4984	0.0544	0.0215	0.01359	0.00878	-3.785	0.02911	14.83	15.17	4.67	2.67
Ensembles	0.6250	0.4693	1.6046	0.0460	0.01343	0.00667	-1.028	0.06199	8.17	8.67	13.50	14.00
Uni-Mol												
Deterministic	0.6079	0.4509	0.8975	0.0425	0.00962	0.00538	0.014	0.06637	5.83	4.83	16.67	21.17
MC Dropout	0.5983	0.4438	1.3663	0.0440	0.00961	0.00535	-0.251	0.06615	4.00	3.17	16.67	21.33
SWAG	0.6026	0.4476	1.0101	0.0453	0.00969	0.00541	-0.462	0.06597	6.33	6.17	19.67	22.67
BBP	0.6044	0.4469	0.0679	0.0306	0.00952	0.00544	-2.959	0.06179	3.17	3.00	4.33	10.33
SGLD	0.6040	0.4554	0.1565	0.0329	0.00950	0.00546	-4.209	0.04593	2.50	4.00	2.50	9.17
Ensembles	0.5809	0.4266	0.6450	0.0438	0.00948	0.00526	-0.319	0.06629	2.50	1.83	11.00	20.67

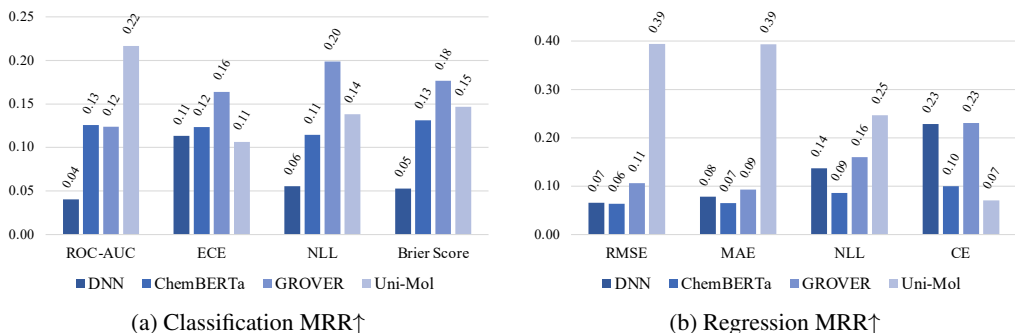


Figure 2: MRR of each backbone model for each metric on classification and regression datasets, respectively. Each MRR is macro-averaged from the reciprocal ranks of the results of all corresponding UQ methods on all datasets.

model with corresponding UQ reciprocal ranks averaged. Compared to the mean ranks displayed in the tables, MRRs accentuate higher-ranked results, offering an alternate perspective on the performance. Our analysis initiates with how the uncertainty estimation contributes to the model prediction, followed by an exploration of the uncertainty quantification performance.

5.1 Prediction Performance

The columns ROC-AUC, RMSE, and MAE in Tables 1, 2, and Figure 2 illustrate the predictive performance of each method. Examining these from the lens of UQ methods, it is noteworthy that despite reported performance gains over direct prediction in their respective papers, no method provides a consistent guarantee of such improvements, except for deep ensembles, and MC Dropout in the case of regression. Deep ensembles effectively explore diverse training modes via random initialization, thus converging more easily to different model optima and mitigating potential distribution gaps

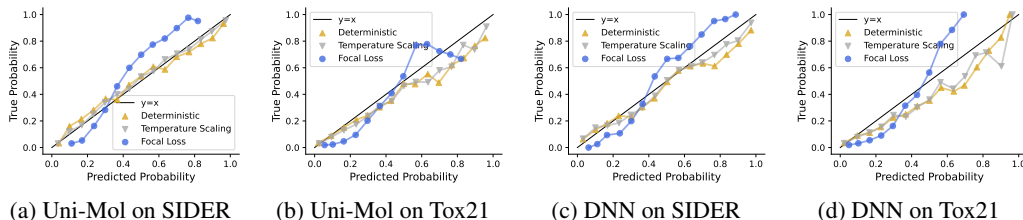


Figure 3: Calibration plot of example uncertainty estimation results. For both datasets, we draw the calibration based on the aggregated outputs from *all* tasks.

between training and test data. MC Dropout’s strategy of enabling dropout during the inference stage of deterministic prediction models parallels the sampling of model parameters from a central multivariate Gaussian distribution based on deterministic net weights. In the context of regression, the aggregation of multiple weight samples may alleviate issues arising from out-of-distribution features triggering extreme output values. However, this mitigation is less pronounced for classification due to output constraints within the $(0, 1)$ range. SWAG, while similar to MC Dropout during training, might intensify training data overfitting due to additional steps taken to fit the parameter distribution, particularly when scaffold splitting intentionally widens training-test deviation. The stochastic sampling employed by BBP and SGLD complicates network training, especially for larger models, impacting their prediction performance as a result.

Looking at these results from the perspective of backbone models, Uni-Mol outperforms other models across the benchmark, securing the best prediction performance for both classification and regression. The superior molecular representation capability of Uni-Mol is attributed to the integration of 3D molecule conformations, a range of pre-training tasks, and a large number of network parameters. When contrasting DNN, ChemBERTa, and GROVER, it becomes apparent that the expressiveness of the molecular descriptors varies for different molecules/tasks. Interestingly, pre-trained models do not invariably surpass heuristic features when integrated with UQ methods. Selecting a model attuned to the specific task is advised over an indiscriminate reliance on “deep and complex” networks.

5.2 Uncertainty Quantification Performance

Tables 1 and 2, along with Figure 2, depict the uncertainty estimation performances via ECE, NLL, Brier score, and CE columns. One discernible trend is the consistent, reliable performance enhancement provided by deep ensembles, even when few ensemble models are deployed in learning processes, such as in the case of QM9. Despite a marginal compromise in prediction accuracy, temperature scaling emerges as another method that almost invariably improves calibration, as evidenced in the average ranking columns—a finding that aligns with those in [27]. We observe from Figure 3 that deterministic prediction tends to be over-confident, and temperature scaling mitigates this issue. An exception is noted in the ToxCast dataset, likely attributable to the distribution deviation between calibration and test datasets. In contrast, Focal loss does not deliver as impressive results, a trend also observed in [55] for binary classification. It is hypothesized that while the Sigmoid function sufficiently captures model confidence in binary cases, Focal loss could over-regularize parameters, diminishing the prediction “sharpness” to an unreasonable value, a conjecture verified by the ‘S’-shaped calibration curves from Focal loss in Figure 3.

Despite their limited efficacy for classification, both BBP and SGLD deliver commendable performance in regression uncertainty prediction, capturing 7 out of 8 top rankings for 4 backbone models with 2 uncertainty metrics, and narrowly missing out to deep ensembles for the remaining one (Table 2, final two columns). Yet, their inconsistent improvement of RMSE and MAE implies a greater influence on variance prediction than mean, corroborated by Figure 4. A striking observation is SGLD’s tendency to “take risks” by predicting smaller variances, while deterministic prediction routinely ascribes large variances even to its accurate predictions. Furthermore, SGLD demonstrates superior error-variance correlation, aligning with its notable calibration performance in Table 2. This might be due to the noise introduced in SGLD and BBP training that enables these models to bypass the “safer decisions with larger variance” optima, which, as observed, reduces the training loss when

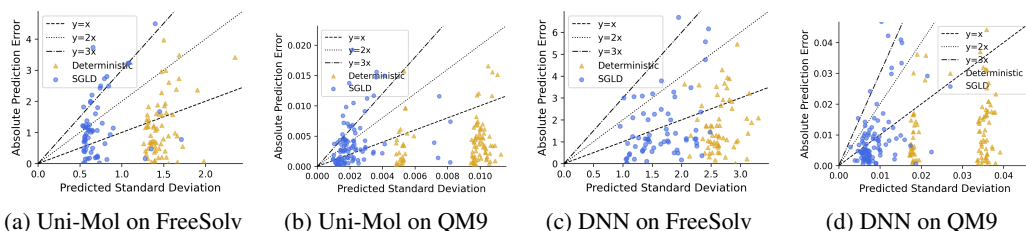


Figure 4: The absolute error between the model-predicted mean and true labels against the predicted standard deviation. We compare the performance of SGLD and deterministic prediction built upon Uni-Mol and DNN on FreeSolv and QM9 (randomly sub-sampled to 200 points) datasets, respectively. The “ $y = kx$ ” lines indicate whether the true labels lie within the k -std range of the predicted Gaussian and also serve as a sign of how errors and variances are correlated. A model is perfectly calibrated when all of its output points are arranged on an “ $y = kx$ ” line for an arbitrary k .

Gaussian NLL is the objective. Other UQ methods encounter the same limitation as deterministic prediction owing to inadequate training randomness.

Figure 2 reveals that Uni-Mol exhibits subpar calibration, particularly for regression. Comparing the subfigures presenting the Uni-Mol and DNN results in Figure 4, it becomes evident that a smaller proportion of Uni-Mol data points fall below the $y = kx$ line for an arbitrary k , suggesting that Uni-Mol is overly confident in its prediction on out-of-distribution features. This could be attributed to shared structural features in 3D conformations in the training and test molecules that remain unobserved in 2D, SMILES, or heuristic representation. While this similarity benefits property prediction, it also potentially misleads the model into considering data points as in-distribution, thereby erroneously assigning high confidence.

6 Conclusion, Limitation, and Future Works

We introduce MUBen, a benchmark that assesses an array of UQ methods across diverse categories, leveraging backbone models that incorporate different molecular descriptors for MoleculeNet’s classification and regression tasks. Our results indicate that while 3D conformations excel in identifying similarities between molecules, they can also result in overconfident and poorly-calibrated models. Although 2D structures are less expressive, they outperform SMILES strings by integrating spatial topology, which is absent in SMILES. In certain instances, pre-trained models do not necessarily yield superior results compared to DNNs trained with heuristic features. In the realm of uncertainty quantification, deep ensembles, as a classic method, assure performance enhancement at the cost of intensive training resource consumption. Alternative methods, although more economical, exhibit limitations in their range of application. If a model has been deterministically trained, our analysis suggests that MC Dropout emerges as a superior option to enhance prediction quality and calibration, requiring only minimal additional resource consumption. For classification tasks, employing temperature scaling provides a straightforward, yet effective strategy to ameliorate calibration, although it marginally compromises prediction accuracy. Conversely, for regression tasks, Stochastic Gradient Langevin Dynamics (SGLD) emerges as a method worth exploring due to its promising potential.

Given the rapid advancements in both molecular representation learning and UQ methods, MUBen cannot possibly encompass all developments so we focus on results from a curated selection of representative methods. Furthermore, the model hyperparameters are fine-tuned with coarse-grained grids to maintain experimental feasibility. This means that the results presented here, while indicative of trends, might not represent the best possible performance. We remain committed to refining MUBen and welcome contributions from the broader community to enhance its inclusivity and utility for research in this field and related domains.

Acknowledgments and Disclosure of Funding

This work was supported in part by ONR MURI N00014-17-1-2656, NSF IIS-2008334, IIS-2106961, and CAREER IIS-2144338.

References

- [1] W. Ahmad, E. Simon, S. Chithrananda, G. Grand, and B. Ramsundar. Chemberta-2: Towards chemical foundation models. *CoRR*, abs/2209.01712, 2022.
- [2] A. Amini, W. Schwarting, A. Soleimany, and D. Rus. Deep evidential regression. In H. Larochelle, M. Ranzato, R. Hadsell, M. Balcan, and H. Lin, editors, *Advances in Neural Information Processing Systems 33: Annual Conference on Neural Information Processing Systems 2020, NeurIPS 2020, December 6-12, 2020, virtual*, 2020.
- [3] S. Amiri, M. S. Shirazi, and S. Zhang. Learning and reasoning for robot sequential decision making under uncertainty. In *Proceedings of the AAAI Conference on Artificial Intelligence*, volume 34, pages 2726–2733, 2020.
- [4] A. N. Angelopoulos and S. Bates. A gentle introduction to conformal prediction and distribution-free uncertainty quantification. *CoRR*, abs/2107.07511, 2021.
- [5] A. N. Angelopoulos, S. Bates, M. I. Jordan, and J. Malik. Uncertainty sets for image classifiers using conformal prediction. In *9th International Conference on Learning Representations, ICLR 2021, Virtual Event, Austria, May 3-7, 2021*. OpenReview.net, 2021.
- [6] C. Blundell, J. Cornebise, K. Kavukcuoglu, and D. Wierstra. Weight uncertainty in neural networks. *CoRR*, abs/1505.05424, 2015.
- [7] G. W. BRIER. Verification of forecasts expressed in terms of probability. *Monthly Weather Review*, 78(1):1–3, Jan. 1950.
- [8] J. Busk, P. B. Jørgensen, A. Bhowmik, M. N. Schmidt, O. Winther, and T. Vegge. Calibrated uncertainty for molecular property prediction using ensembles of message passing neural networks. *Machine Learning: Science and Technology*, 3(1):015012, 2021.
- [9] H. Chen, Y. Huang, W. Tian, Z. Gao, and L. Xiong. Monorun: Monocular 3d object detection by reconstruction and uncertainty propagation. In *Proceedings of the IEEE/CVF Conference on Computer Vision and Pattern Recognition*, pages 10379–10388, 2021.
- [10] S. Chithrananda, G. Grand, and B. Ramsundar. Chemberta: Large-scale self-supervised pretraining for molecular property prediction. *CoRR*, abs/2010.09885, 2020.
- [11] A. C. Damianou and N. D. Lawrence. Deep gaussian processes. In *Proceedings of the Sixteenth International Conference on Artificial Intelligence and Statistics, AISTATS 2013, Scottsdale, AZ, USA, April 29 - May 1, 2013*, volume 31 of *JMLR Workshop and Conference Proceedings*, pages 207–215. JMLR.org, 2013.
- [12] A. Deshwal, C. M. Simon, and J. R. Doppa. Bayesian optimization of nanoporous materials. *Molecular Systems Design & Engineering*, 6(12):1066–1086, 2021.
- [13] J. Devlin, M. Chang, K. Lee, and K. Toutanova. BERT: pre-training of deep bidirectional transformers for language understanding. In J. Burstein, C. Doran, and T. Solorio, editors, *Proceedings of the 2019 Conference of the North American Chapter of the Association for Computational Linguistics: Human Language Technologies, NAACL-HLT 2019, Minneapolis, MN, USA, June 2-7, 2019, Volume 1 (Long and Short Papers)*, pages 4171–4186. Association for Computational Linguistics, 2019.
- [14] T. G. Dietterich. Ensemble methods in machine learning. In J. Kittler and F. Roli, editors, *Multiple Classifier Systems, First International Workshop, MCS 2000, Cagliari, Italy, June 21-23, 2000, Proceedings*, volume 1857 of *Lecture Notes in Computer Science*, pages 1–15. Springer, 2000.
- [15] N. S. Eyke, W. H. Green, and K. F. Jensen. Iterative experimental design based on active machine learning reduces the experimental burden associated with reaction screening. *React. Chem. Eng.*, 5:1963–1972, 2020.
- [16] X. Fang, L. Liu, J. Lei, D. He, S. Zhang, J. Zhou, F. Wang, H. Wu, and H. Wang. Geometry-enhanced molecular representation learning for property prediction. *Nat. Mach. Intell.*, 4(2):127–134, 2022.
- [17] S. Fort, H. Hu, and B. Lakshminarayanan. Deep ensembles: A loss landscape perspective. *CoRR*, abs/1912.02757, 2019.

- [18] Y. Gal and Z. Ghahramani. Dropout as a bayesian approximation: Representing model uncertainty in deep learning. In M. Balcan and K. Q. Weinberger, editors, *Proceedings of the 33rd International Conference on Machine Learning, ICML 2016, New York City, NY, USA, June 19-24, 2016*, volume 48 of *JMLR Workshop and Conference Proceedings*, pages 1050–1059. JMLR.org, 2016.
- [19] Y. Gal, R. Islam, and Z. Ghahramani. Deep bayesian active learning with image data. In D. Precup and Y. W. Teh, editors, *Proceedings of the 34th International Conference on Machine Learning, ICML 2017, Sydney, NSW, Australia, 6-11 August 2017*, volume 70 of *Proceedings of Machine Learning Research*, pages 1183–1192. PMLR, 2017.
- [20] A. Gaulton, L. J. Bellis, A. P. Bento, J. Chambers, M. Davies, A. Hersey, Y. Light, S. McGlinchey, D. Michalovich, B. Al-Lazikani, et al. ChEMBL: a large-scale bioactivity database for drug discovery. *Nucleic acids research*, 40(D1):D1100–D1107, 2012.
- [21] J. Gawlikowski, C. R. N. Tassi, M. Ali, J. Lee, M. Humt, J. Feng, A. M. Kruspe, R. Triebel, P. Jung, R. Roscher, M. Shahzad, W. Yang, R. Bamler, and X. X. Zhu. A survey of uncertainty in deep neural networks. *CoRR*, abs/2107.03342, 2021.
- [22] Y. Geifman and R. El-Yaniv. Selective classification for deep neural networks. In I. Guyon, U. von Luxburg, S. Bengio, H. M. Wallach, R. Fergus, S. V. N. Vishwanathan, and R. Garnett, editors, *Advances in Neural Information Processing Systems 30: Annual Conference on Neural Information Processing Systems 2017, December 4-9, 2017, Long Beach, CA, USA*, pages 4878–4887, 2017.
- [23] J. Gilmer, S. S. Schoenholz, P. F. Riley, O. Vinyals, and G. E. Dahl. Neural message passing for quantum chemistry. In D. Precup and Y. W. Teh, editors, *Proceedings of the 34th International Conference on Machine Learning, ICML 2017, Sydney, NSW, Australia, 6-11 August 2017*, volume 70 of *Proceedings of Machine Learning Research*, pages 1263–1272. PMLR, 2017.
- [24] T. Gneiting and A. E. Raftery. Strictly proper scoring rules, prediction, and estimation. *Journal of the American Statistical Association*, 102(477):359–378, Mar. 2007.
- [25] K. P. Greenman, A. Soleimany, and K. K. Yang. Benchmarking uncertainty quantification for protein engineering. In *ICLR2022 Machine Learning for Drug Discovery, 2022*.
- [26] C. J. Gruich, V. Madhavan, Y. Wang, and B. R. Goldsmith. Clarifying trust of materials property predictions using neural networks with distribution-specific uncertainty quantification. *Machine Learning: Science and Technology*, 4(2):025019, 2023.
- [27] C. Guo, G. Pleiss, Y. Sun, and K. Q. Weinberger. On calibration of modern neural networks. In D. Precup and Y. W. Teh, editors, *Proceedings of the 34th International Conference on Machine Learning, ICML 2017, Sydney, NSW, Australia, 6-11 August 2017*, volume 70 of *Proceedings of Machine Learning Research*, pages 1321–1330. PMLR, 2017.
- [28] Y. He, C. Zhu, J. Wang, M. Savvides, and X. Zhang. Bounding box regression with uncertainty for accurate object detection. In *Proceedings of the IEEE/CVF Conference on Computer Vision and Pattern Recognition*, pages 2888–2897, 2019.
- [29] D. Hendrycks and K. Gimpel. Gaussian error linear units (gelus), 2016.
- [30] G. E. Hinton, O. Vinyals, and J. Dean. Distilling the knowledge in a neural network. *CoRR*, abs/1503.02531, 2015.
- [31] L. Hirschfeld, K. Swanson, K. Yang, R. Barzilay, and C. W. Coley. Uncertainty quantification using neural networks for molecular property prediction. *Journal of Chemical Information and Modeling*, 60(8):3770–3780, 2020. PMID: 32702986.
- [32] W. Hu, B. Liu, J. Gomes, M. Zitnik, P. Liang, V. S. Pande, and J. Leskovec. Strategies for pre-training graph neural networks. In *8th International Conference on Learning Representations, ICLR 2020, Addis Ababa, Ethiopia, April 26-30, 2020*. OpenReview.net, 2020.
- [33] K. Huang, V. Sresht, B. K. Rai, and M. Bordyuh. Uncertainty-aware pseudo-labeling for quantum calculations. In J. Cussens and K. Zhang, editors, *Uncertainty in Artificial Intelligence, Proceedings of the Thirty-Eighth Conference on Uncertainty in Artificial Intelligence, UAI 2022, 1-5 August 2022, Eindhoven, The Netherlands*, volume 180 of *Proceedings of Machine Learning Research*, pages 853–862. PMLR, 2022.
- [34] D. Hwang, G. Lee, H. Jo, S. Yoon, and S. Ryu. A benchmark study on reliable molecular supervised learning via bayesian learning. *CoRR*, abs/2006.07021, 2020.

- [35] P. Izmailov, D. Podoprikin, T. Garipov, D. P. Vetrov, and A. G. Wilson. Averaging weights leads to wider optima and better generalization. In A. Globerson and R. Silva, editors, *Proceedings of the Thirty-Fourth Conference on Uncertainty in Artificial Intelligence, UAI 2018, Monterey, California, USA, August 6-10, 2018*, pages 876–885. AUAI Press, 2018.
- [36] Z. Jiang, J. Araki, H. Ding, and G. Neubig. How can we know when language models know? on the calibration of language models for question answering. *Transactions of the Association for Computational Linguistics*, 9:962–977, 2021.
- [37] H. Kamarthi, L. Kong, A. Rodríguez, C. Zhang, and B. A. Prakash. When in doubt: Neural non-parametric uncertainty quantification for epidemic forecasting. In M. Ranzato, A. Beygelzimer, Y. N. Dauphin, P. Liang, and J. W. Vaughan, editors, *Advances in Neural Information Processing Systems 34: Annual Conference on Neural Information Processing Systems 2021, NeurIPS 2021, December 6-14, 2021, virtual*, pages 19796–19807, 2021.
- [38] D. Kim, J. Baek, and S. J. Hwang. Graph self-supervised learning with accurate discrepancy learning. In *NeurIPS*, 2022.
- [39] M. Kim, M. Y. Ha, W.-B. Jung, J. Yoon, E. Shin, I.-d. Kim, W. B. Lee, Y. Kim, and H.-t. Jung. Searching for an optimal multi-metallic alloy catalyst by active learning combined with experiments. *Advanced Materials*, 34(19):2108900, 2022.
- [40] D. P. Kingma, T. Salimans, and M. Welling. Variational dropout and the local reparameterization trick. In C. Cortes, N. D. Lawrence, D. D. Lee, M. Sugiyama, and R. Garnett, editors, *Advances in Neural Information Processing Systems 28: Annual Conference on Neural Information Processing Systems 2015, December 7-12, 2015, Montreal, Quebec, Canada*, pages 2575–2583, 2015.
- [41] D. P. Kingma and M. Welling. Auto-encoding variational bayes. In Y. Bengio and Y. LeCun, editors, *2nd International Conference on Learning Representations, ICLR 2014, Banff, AB, Canada, April 14-16, 2014, Conference Track Proceedings*, 2014.
- [42] L. Kong, J. Cui, Y. Zhuang, R. Feng, B. A. Prakash, and C. Zhang. End-to-end stochastic optimization with energy-based model. In *NeurIPS*, 2022.
- [43] L. Kong, H. Jiang, Y. Zhuang, J. Lyu, T. Zhao, and C. Zhang. Calibrated language model fine-tuning for in- and out-of-distribution data. In B. Webber, T. Cohn, Y. He, and Y. Liu, editors, *Proceedings of the 2020 Conference on Empirical Methods in Natural Language Processing, EMNLP 2020, Online, November 16-20, 2020*, pages 1326–1340. Association for Computational Linguistics, 2020.
- [44] V. Kuleshov, N. Fenner, and S. Ermon. Accurate uncertainties for deep learning using calibrated regression. In J. G. Dy and A. Krause, editors, *Proceedings of the 35th International Conference on Machine Learning, ICML 2018, Stockholmsmässan, Stockholm, Sweden, July 10-15, 2018*, volume 80 of *Proceedings of Machine Learning Research*, pages 2801–2809. PMLR, 2018.
- [45] B. Lakshminarayanan, A. Pritzel, and C. Blundell. Simple and scalable predictive uncertainty estimation using deep ensembles. In I. Guyon, U. von Luxburg, S. Bengio, H. M. Wallach, R. Fergus, S. V. N. Vishwanathan, and R. Garnett, editors, *Advances in Neural Information Processing Systems 30: Annual Conference on Neural Information Processing Systems 2017, December 4-9, 2017, Long Beach, CA, USA*, pages 6402–6413, 2017.
- [46] P. Li, J. Wang, Y. Qiao, H. Chen, Y. Yu, X. Yao, P. Gao, G. Xie, and S. Song. An effective self-supervised framework for learning expressive molecular global representations to drug discovery. *Briefings in Bioinformatics*, 22(6):bbab109, 2021.
- [47] T. Lin, P. Goyal, R. B. Girshick, K. He, and P. Dollár. Focal loss for dense object detection. In *IEEE International Conference on Computer Vision, ICCV 2017, Venice, Italy, October 22-29, 2017*, pages 2999–3007. IEEE Computer Society, 2017.
- [48] S. Liu, H. Wang, W. Liu, J. Lasenby, H. Guo, and J. Tang. Pre-training molecular graph representation with 3d geometry. In *The Tenth International Conference on Learning Representations, ICLR 2022, Virtual Event, April 25-29, 2022*. OpenReview.net, 2022.
- [49] Y. Liu, M. Ott, N. Goyal, J. Du, M. Joshi, D. Chen, O. Levy, M. Lewis, L. Zettlemoyer, and V. Stoyanov. Roberta: A robustly optimized BERT pretraining approach. *CoRR*, abs/1907.11692, 2019.

- [50] I. Loshchilov and F. Hutter. Decoupled weight decay regularization. In *7th International Conference on Learning Representations, ICLR 2019, New Orleans, LA, USA, May 6-9, 2019*. OpenReview.net, 2019.
- [51] W. J. Maddox, P. Izmailov, T. Garipov, D. P. Vetrov, and A. G. Wilson. A simple baseline for bayesian uncertainty in deep learning. In H. M. Wallach, H. Larochelle, A. Beygelzimer, F. d’Alché-Buc, E. B. Fox, and R. Garnett, editors, *Advances in Neural Information Processing Systems 32: Annual Conference on Neural Information Processing Systems 2019, NeurIPS 2019, December 8-14, 2019, Vancouver, BC, Canada*, pages 13132–13143, 2019.
- [52] O. Mamun, K. T. Winther, J. R. Boes, and T. Bligaard. A bayesian framework for adsorption energy prediction on bimetallic alloy catalysts. *npj Computational Materials*, 6(1):177, 2020.
- [53] H. L. Morgan. The generation of a unique machine description for chemical structures—a technique developed at chemical abstracts service. *Journal of Chemical Documentation*, 5(2):107–113, 1965.
- [54] S. Mukherjee and A. Awadallah. Uncertainty-aware self-training for few-shot text classification. *Advances in Neural Information Processing Systems*, 33:21199–21212, 2020.
- [55] J. Mukhoti, V. Kulharia, A. Sanyal, S. Golodetz, P. H. S. Torr, and P. K. Dokania. Calibrating deep neural networks using focal loss. In H. Larochelle, M. Ranzato, R. Hadsell, M. Balcan, and H. Lin, editors, *Advances in Neural Information Processing Systems 33: Annual Conference on Neural Information Processing Systems 2020*, 2020.
- [56] A. H. Murphy. A new vector partition of the probability score. *Journal of Applied Meteorology and Climatology*, 12(4):595–600, 1973.
- [57] M. P. Naeini, G. Cooper, and M. Hauskrecht. Obtaining well calibrated probabilities using bayesian binning. In *AAAI Conference on Artificial Intelligence*, 29(1), Feb. 2015.
- [58] J. Noh, G. H. Gu, S. Kim, and Y. Jung. Uncertainty-quantified hybrid machine learning/density functional theory high throughput screening method for crystals. *Journal of Chemical Information and Modeling*, 60(4):1996–2003, 2020.
- [59] A. Paszke, S. Gross, F. Massa, A. Lerer, J. Bradbury, G. Chanan, T. Killeen, Z. Lin, N. Gimelshein, L. Antiga, A. Desmaison, A. Köpf, E. Z. Yang, Z. DeVito, M. Raison, A. Tejani, S. Chilamkurthy, B. Steiner, L. Fang, J. Bai, and S. Chintala. Pytorch: An imperative style, high-performance deep learning library. In H. M. Wallach, H. Larochelle, A. Beygelzimer, F. d’Alché-Buc, E. B. Fox, and R. Garnett, editors, *Advances in Neural Information Processing Systems 32: Annual Conference on Neural Information Processing Systems 2019, NeurIPS 2019, December 8-14, 2019, Vancouver, BC, Canada*, pages 8024–8035, 2019.
- [60] J. Platt et al. Probabilistic outputs for support vector machines and comparisons to regularized likelihood methods. *Advances in large margin classifiers*, 10(3):61–74, 1999.
- [61] S. Qin, J. Zhu, J. Qin, W. Wang, and D. Zhao. Recurrent attentive neural process for sequential data. *arXiv preprint arXiv:1910.09323*, 2019.
- [62] J. Quiñero-Candela, C. E. Rasmussen, F. Sinz, O. Bousquet, and B. Schölkopf. Evaluating predictive uncertainty challenge. In *Machine Learning Challenges. Evaluating Predictive Uncertainty, Visual Object Classification, and Recognising Tectual Entailment*, pages 1–27. Springer Berlin Heidelberg, 2006.
- [63] A. Radford, K. Narasimhan, T. Salimans, and I. Sutskever. Improving language understanding with unsupervised learning. 2018.
- [64] Y. Rong, Y. Bian, T. Xu, W. Xie, Y. Wei, W. Huang, and J. Huang. Self-supervised graph transformer on large-scale molecular data. In H. Larochelle, M. Ranzato, R. Hadsell, M. Balcan, and H. Lin, editors, *Advances in Neural Information Processing Systems 33: Annual Conference on Neural Information Processing Systems 2020, NeurIPS 2020, December 6-12, 2020, virtual*, 2020.
- [65] J. Ross, B. Belgodere, V. Chenthamarakshan, I. Padhi, Y. Mroueh, and P. Das. Large-scale chemical language representations capture molecular structure and properties. *Nat. Mac. Intell.*, 4(12):1256–1264, 2022.
- [66] G. Scalia, C. A. Grambow, B. Pernici, Y.-P. Li, and W. H. Green. Evaluating scalable uncertainty estimation methods for deep learning-based molecular property prediction. *Journal of chemical information and modeling*, 60(6):2697–2717, 2020.

- [67] P. Schwaller, T. Laino, T. Gaudin, P. Bolgar, C. A. Hunter, C. Bekas, and A. A. Lee. Molecular transformer: A model for uncertainty-calibrated chemical reaction prediction. *ACS Central Science*, 5(9):1572–1583, 2019. PMID: 31572784.
- [68] M. Sensoy, L. M. Kaplan, and M. Kandemir. Evidential deep learning to quantify classification uncertainty. In S. Bengio, H. M. Wallach, H. Larochelle, K. Grauman, N. Cesa-Bianchi, and R. Garnett, editors, *Advances in Neural Information Processing Systems 31: Annual Conference on Neural Information Processing Systems 2018, NeurIPS 2018, December 3-8, 2018, Montréal, Canada*, pages 3183–3193, 2018.
- [69] A. P. Soleimany, A. Amini, S. Goldman, D. Rus, S. N. Bhatia, and C. W. Coley. Evidential deep learning for guided molecular property prediction and discovery. *ACS Central Science*, 7(8):1356–1367, 2021.
- [70] H. Song, T. Diethe, M. Kull, and P. A. Flach. Distribution calibration for regression. In K. Chaudhuri and R. Salakhutdinov, editors, *Proceedings of the 36th International Conference on Machine Learning, ICML 2019, 9-15 June 2019, Long Beach, California, USA*, volume 97 of *Proceedings of Machine Learning Research*, pages 5897–5906. PMLR, 2019.
- [71] N. Srivastava, G. E. Hinton, A. Krizhevsky, I. Sutskever, and R. Salakhutdinov. Dropout: a simple way to prevent neural networks from overfitting. *J. Mach. Learn. Res.*, 15(1):1929–1958, 2014.
- [72] H. Stärk, D. Beaini, G. Corso, P. Tossou, C. Dallago, S. Günnemann, and P. Lió. 3d infomax improves gnn for molecular property prediction. In K. Chaudhuri, S. Jegelka, L. Song, C. Szepesvári, G. Niu, and S. Sabato, editors, *International Conference on Machine Learning, ICML 2022, 17-23 July 2022, Baltimore, Maryland, USA*, volume 162 of *Proceedings of Machine Learning Research*, pages 20479–20502. PMLR, 2022.
- [73] T. Sterling and J. J. Irwin. Zinc 15 - ligand discovery for everyone. *Journal of Chemical Information and Modeling*, 55(11):2324–2337, 2015. PMID: 26479676.
- [74] F. Sun, J. Hoffmann, V. Verma, and J. Tang. Infograph: Unsupervised and semi-supervised graph-level representation learning via mutual information maximization. In *8th International Conference on Learning Representations, ICLR 2020, Addis Ababa, Ethiopia, April 26-30, 2020*. OpenReview.net, 2020.
- [75] Q. Tan, M. Ye, A. J. Ma, B. Yang, T. C.-F. Yip, G. L.-H. Wong, and P. C. Yuen. Explainable uncertainty-aware convolutional recurrent neural network for irregular medical time series. *IEEE Transactions on Neural Networks and Learning Systems*, 32(10):4665–4679, 2020.
- [76] A. Vaswani, N. Shazeer, N. Parmar, J. Uszkoreit, L. Jones, A. N. Gomez, L. Kaiser, and I. Polosukhin. Attention is all you need. In I. Guyon, U. von Luxburg, S. Bengio, H. M. Wallach, R. Fergus, S. V. N. Vishwanathan, and R. Garnett, editors, *Advances in Neural Information Processing Systems 30: Annual Conference on Neural Information Processing Systems 2017, December 4-9, 2017, Long Beach, CA, USA*, pages 5998–6008, 2017.
- [77] W. P. Walters and R. Barzilay. Applications of deep learning in molecule generation and molecular property prediction. *Accounts of Chemical Research*, 54(2):263–270, 2021. PMID: 33370107.
- [78] S. Wang, Y. Guo, Y. Wang, H. Sun, and J. Huang. SMILES-BERT: large scale unsupervised pre-training for molecular property prediction. In X. M. Shi, M. Buck, J. Ma, and P. Veltri, editors, *Proceedings of the 10th ACM International Conference on Bioinformatics, Computational Biology and Health Informatics, BCB 2019, Niagara Falls, NY, USA, September 7-10, 2019*, pages 429–436. ACM, 2019.
- [79] Y. Wang, J. Wang, Z. Cao, and A. Barati Farimani. Molecular contrastive learning of representations via graph neural networks. *Nature Machine Intelligence*, 4(3):279–287, 2022.
- [80] Y. Wang, J. Xiao, T. O. Suzek, J. Zhang, J. Wang, and S. H. Bryant. Pubchem: a public information system for analyzing bioactivities of small molecules. *Nucleic Acids Res.*, 37(Web-Server-Issue):623–633, 2009.
- [81] D. Weininger. Smiles, a chemical language and information system. 1. introduction to methodology and encoding rules. *Journal of Chemical Information and Computer Sciences*, 28(1):31–36, 1988.

- [82] M. Welling and Y. W. Teh. Bayesian learning via stochastic gradient langevin dynamics. In L. Getoor and T. Scheffer, editors, *Proceedings of the 28th International Conference on Machine Learning, ICML 2011, Bellevue, Washington, USA, June 28 - July 2, 2011*, pages 681–688. Omnipress, 2011.
- [83] T. Wolf, L. Debut, V. Sanh, J. Chaumond, C. Delangue, A. Moi, P. Cistac, T. Rault, R. Louf, M. Funtowicz, and J. Brew. Huggingface’s transformers: State-of-the-art natural language processing. *CoRR*, abs/1910.03771, 2019.
- [84] Z. Wu, B. Ramsundar, E. N. Feinberg, J. Gomes, C. Geniesse, A. S. Pappu, K. Leswing, and V. Pande. Moleculenet: a benchmark for molecular machine learning. *Chemical Science*, 9(2):513–530, 2018.
- [85] J. Xia, Y. Zhu, Y. Du, Y. Liu, and S. Z. Li. A systematic survey of molecular pre-trained models. *CoRR*, abs/2210.16484, 2022.
- [86] K. Yang, K. Swanson, W. Jin, C. Coley, P. Eiden, H. Gao, A. Guzman-Perez, T. Hopper, B. Kelley, M. Mathea, A. Palmer, V. Settels, T. Jaakkola, K. Jensen, and R. Barzilay. Correction to analyzing learned molecular representations for property prediction. *Journal of Chemical Information and Modeling*, 59(12):5304–5305, 2019. PMID: 31814400.
- [87] Y. You, T. Chen, Y. Sui, T. Chen, Z. Wang, and Y. Shen. Graph contrastive learning with augmentations. In H. Larochelle, M. Ranzato, R. Hadsell, M. Balcan, and H. Lin, editors, *Advances in Neural Information Processing Systems 33: Annual Conference on Neural Information Processing Systems 2020, NeurIPS 2020, December 6-12, 2020, virtual*, 2020.
- [88] Y. Yu, L. Kong, J. Zhang, R. Zhang, and C. Zhang. Actune: Uncertainty-based active self-training for active fine-tuning of pretrained language models. In *Proceedings of the 2022 Conference of the North American Chapter of the Association for Computational Linguistics: Human Language Technologies*, pages 1422–1436, 2022.
- [89] C. Zhang, Y. Amar, L. Cao, and A. A. Lapkin. Solvent selection for mitsunobu reaction driven by an active learning surrogate model. *Organic Process Research & Development*, 24(12):2864–2873, 2020.
- [90] G. Zhou, Z. Gao, Q. Ding, H. Zheng, H. Xu, Z. Wei, L. Zhang, and G. Ke. Uni-mol: A universal 3d molecular representation learning framework. In *The Eleventh International Conference on Learning Representations*, 2023.

Checklist

1. For all authors...
 - (a) Do the main claims made in the abstract and introduction accurately reflect the paper’s contributions and scope? [\[Yes\]](#)
 - (b) Did you describe the limitations of your work? [\[Yes\]](#) sec:conclusion
 - (c) Did you discuss any potential negative societal impacts of your work? [\[N/A\]](#)
 - (d) Have you read the ethics review guidelines and ensured that your paper conforms to them? [\[Yes\]](#)
2. If you are including theoretical results...
 - (a) Did you state the full set of assumptions of all theoretical results? [\[N/A\]](#)
 - (b) Did you include complete proofs of all theoretical results? [\[N/A\]](#)
3. If you ran experiments (e.g. for benchmarks)...
 - (a) Did you include the code, data, and instructions needed to reproduce the main experimental results (either in the supplemental material or as a URL)? [\[Yes\]](#) See § 1
 - (b) Did you specify all the training details (e.g., data splits, hyperparameters, how they were chosen)? [\[Yes\]](#) See § 4 and appendix
 - (c) Did you report error bars (e.g., with respect to the random seed after running experiments multiple times)? [\[Yes\]](#) See appendix
 - (d) Did you include the total amount of compute and the type of resources used (e.g., type of GPUs, internal cluster, or cloud provider)? [\[Yes\]](#) See appendix
4. If you are using existing assets (e.g., code, data, models) or curating/releasing new assets...

- (a) If your work uses existing assets, did you cite the creators? [Yes] See § 4 and appendix
 - (b) Did you mention the license of the assets? [Yes] See appendix
 - (c) Did you include any new assets either in the supplemental material or as a URL? [Yes] See § 1
 - (d) Did you discuss whether and how consent was obtained from people whose data you're using/curating? [N/A]
 - (e) Did you discuss whether the data you are using/curating contains personally identifiable information or offensive content? [N/A]
5. If you used crowdsourcing or conducted research with human subjects...
- (a) Did you include the full text of instructions given to participants and screenshots, if applicable? [N/A]
 - (b) Did you describe any potential participant risks, with links to Institutional Review Board (IRB) approvals, if applicable? [N/A]
 - (c) Did you include the estimated hourly wage paid to participants and the total amount spent on participant compensation? [N/A]

Table 3: Dataset statistics in MUBen.

Task Type	Dataset	# Compounds	# Tasks	Average LIR ^a	Max LIR ^b
Classification	BACE	1,513	1	0.5433	0.5433
	BBBP	2,039	1	0.7651	0.7651
	ClinTox	1,478	2	0.9303	0.9364
	Tox21	7,831	12	0.9225	0.9712
	ToxCast	8,575	617	0.8336	0.9972
	SIDER	1,427	27	0.7485	0.9846
	HIV	41,127	1	0.9649	0.9649
	MUV	93,087	17	0.9980	0.9984
Regression	ESOL	1,128	1	-	-
	FreeSolv	642	1	-	-
	Lipophilicity	4,200	1	-	-
	QM7	7,160	1	-	-
	QM8	21,786	12	-	-
	QM9	133,885	3 ²	-	-

^a LIR stands for "label imbalance ratio", which is calculated as $\text{LIR}_k \in [0.5, 1] = \max\{p_{\text{pos}}, p_{\text{neg}}\}$ for a task indexed by $k \in \{1, \dots, K\}$, where p_{pos} and p_{neg} are the proportions of positive and negative samples in the dataset, respectively. LIR = 0.5 indicates a balanced dataset and LIR = 1 indicates a completely imbalanced one, with either $y = 0$ or $y = 1$ being absent. Average LIR = $\sum_{k=1}^K \text{LIR}_k$, and Max LIR = $\max_k \{\text{LIR}_k\}$. LIR is calculated on the entire dataset, and the number could slightly vary for each partition.

^b Notice that QM9 originally contains 12 tasks, but we only use 3 of them following previous works [16, 90].

A Dataset Details

In this section, we provide details about the datasets used in our study. We follow the approach of previous works [16, 90] and select a subset of widely used and publicly available datasets from the MoleculeNet benchmark [84]. The datasets cover both classification and regression tasks, and we provide a brief description of each below.

- **BACE** provides binary binding properties for a set of inhibitors of human β -secretase 1 (BACE-1) from experimental values from the published papers;
- **BBBP (Blood-Brain Barrier Penetration)** studies the classification of molecules by their permeability of the blood-brain barrier;
- **ClinTox** consists of two classification tasks for drugs: whether they are absent of clinical toxicity and whether they are approved by the FDA;
- **Tox21 (Toxicology in the 21st Century)** consists of qualitative toxicity measurements of 8,014 compounds on 12 different targets;
- **ToxCast** provides toxicology data of 8,576 compounds on 617 different targets;
- **SIDER (Side Effect Resource)** contains marketed drugs and adverse drug reactions (ADR) extracted from package inserts;
- **HIV**, introduced by the Drug Therapeutics Program (DTP) AIDS Antiviral Screen, contains compounds that are either active or inactive against HIV replication;
- **MUV (Maximum Unbiased Validation)**, a challenging benchmark dataset selected from PubChem BioAssay for validation of virtual screening techniques, contains 93,087 compounds tested for activity against 17 different targets.

The regression datasets include:

- **ESOL** provides experimental values for water solubility data for 1,128 compounds;
- **FreeSolv (Free Solvation Database)** contains experimental and calculated hydration free energies for 643 small molecules;

Table 4: Model statistics.

Model	# Parameters (M)	Average Time per Training Step (ms) ¹
DNN	0.158	5.39
ChemBERTa	3.43	30.18
GROVER	48.71	334.47
Uni-Mol	47.59	392.55

¹ All models are evaluated on the BBBP dataset with a batch size of 128. We only measure the time for forward passing, backward passing, and parameter updating. We train the model for 6 epochs and take the average of the last 5.

- **Lipophilicity** contains experimental results of octanol/water distribution coefficient for 4,200 compounds;
- **QM7/8/9** are subsets of GDB-13 and GDB-17 databases containing quantum mechanical calculations of energies, enthalpies, and dipole moments for organic molecules with up to 7/8/9 "heavy" atoms, respectively. For QM9, we follow previous works [16, 90] and select 3 tasks that predict properties (homo, lumo, and gap) with a similar quantitative range out of the total 12.

A summary of the dataset statistics is provided in Table 3. It is worth noting that some datasets, such as HIV and MUV, exhibit a high degree of class imbalance. This characteristic adds further challenges to the tasks of molecular property prediction and uncertainty quantification.

For all datasets, we construct the training, validation, and test subsets using scaffold splitting with an 8:1:1. The raw datasets are available on the MoleculeNet website.¹ We take advantage of the pre-processed version shared by [90] and use the same splits as in their work.²

B Backbone Models and Implementation Details

Our experimental code is designed on the PyTorch framework [59]. The backbone models we use are fine-tuned using the AdamW optimizer [50], which utilizes a weight decay rate of 0.01. Each training process is conducted on a single NVIDIA A100 Tensor Core GPU with a memory capacity of 80GB. We implement early stopping epochs on all models, albeit with varying tolerance epochs. All models have achieved their peak performance on the validation set before the training ends. Table 4 presents the number of parameters and average time per training step for each backbone model. Notice that the training time is calculated for each *step* instead of each epoch based on our implementation, which might be slower than the models' original realizations. Below, we offer a detailed description of each backbone model's architecture and its implementation.

ChemBERTa ChemBERTa [10, 1] leverages the RoBERTa model architecture and pre-training strategy [49] but with fewer layers, attention heads, and smaller hidden dimensionalities. Unlike traditional models which process natural language sentences, ChemBERTa uses Simplified Molecular-Input Line-Entry System (SMILES) strings [81] as input. This representation is a compact and linear textual depiction of a molecule's structure that's frequently employed in cheminformatics. ChemBERTa pre-training adopts a corpus of 77M SMILES strings from PubChem [80], along with the masked language modeling objective [13].

ChemBERTa is built with the HuggingFace Transformers library [83], and its pre-trained parameters are shared through the Huggingface's model hub. We retain the default model architecture identical to BERT-base [13] and RoBERTa-base [49], using the DeepChem/ChemBERTa-77M-MLM checkpoint for ChemBERTa's weight initialization³. We employ the sequence embedding of the [CLS] token to represent the input SMILES and attach a linear output layer for property prediction. During fine-tuning, ChemBERTa models are trained on all datasets with a learning rate of 10^{-5} , using a batch size of 128 for 200 epochs. A tolerance of 40 epochs for early stopping is adopted.

¹<https://moleculenet.org/>

²Repository at <https://github.com/dptech-corp/Uni-Mol/tree/main/unimol> and download at https://bioos-hermite-beijing.tos-cn-beijing.volces.com/unimol_data/finetune/molecular_property_prediction.tar.gz.

³Accessible at <https://huggingface.co/DeepChem/ChemBERTa-77M-MLM>.

GROVER GROVER [64] is pre-trained on 11M unlabeled molecules as 2D molecular graphs from ZINC15 [73] and ChEMBL [20]. To enhance pre-training on molecular graphs, GROVER integrates the graph neural network (GNN)-based Message Passing Neural Networks (MPNN) [23] into the Transformer encoder architectures. It also devises self-supervised objectives from different molecular structural granularities to better capture the rich structural and semantic information of molecules. Specifically, GROVER replaces the linear layer used for mapping the input query, key, and value vectors of each multi-head attention module into the head-dependent latent feature spaces in the Transformer encoder with a dynamic message passing network. This network aggregates the latent features from the k -hop neighboring nodes, where k is a random integer drawn from a pre-defined Uniform of Gaussian. In other words, GROVER puts GNN layers before each head’s self-attention computation to better encode the graph structure of molecules. To facilitate learning, GROVER introduces training objectives including contextual property prediction, which predicts the statistical properties of masked subgraphs of arbitrary sizes, and graph-level motif prediction, which predicts the classes of the masked functional groups. GROVER uses a readout function to aggregate node features, which are then passed into linear layers for property prediction.

For implementation, we use the GROVER-base checkpoint for our model initialization⁴. We incorporate the “node-view” branch as discussed above and disregard the “edge-view” architecture detailed in the appendix of [64], in accordance with the default settings in the GitHub repository. Under this configuration, the model generates 2 sets of node embeddings (but no edge embeddings), one from the node hidden states and another from the edge hidden states [64]. Each set of embeddings is passed into 2 linear layers with GELU [29] activation and a dropout ratio of 0.1 post-readout layer, which simply averages the embeddings in the default configuration. Each set of embeddings corresponds to an individual output branch, predicting the properties independently. In line with the original implementation, we compute the loss for each branch individually during fine-tuning and apply a squared Euclidean distance regularization with a coefficient of 0.1 between the two. During inference, we average the logits from the 2 branches to generate the final output logits.

In our experiments, we configure the fine-tuning batch size at 256, and the number of epochs at 100 with a tolerance of 40 epochs for early stopping. The learning rate is set at 10^{-4} , and the entire model has a dropout ratio of 0.1. We substitute the original Noam learning rate scheduler [76] with a linear learning rate scheduler with a 0.1 warm-up ratio for easier implementation. No substantial differences in model performance were observed between the two learning rate schedulers.

Uni-Mol Uni-Mol [90] is a universal molecular representation framework that enhances representational capacity and broadens applicability by incorporating 3D molecular structures as model input. For the property prediction task, Uni-Mol undergoes pre-training on 209M 3D conformations of organic molecules gathered from ZINC15 [73], ChEMBL [20], and a database comprising 12M purchasable molecules [90]. It portrays atoms as tokens and utilizes pair-type aware Gaussian kernels to encode the positional information in the 3D space, thereby ensuring rotational and translational invariance. Furthermore, Uni-Mol introduces a pair-level representation by orchestrating an “atom-to-pair” communication—updating positional encodings with query-key products—and a “pair-to-atom” communication—adding pair representation as bias terms in the self-attention atom update procedure. For pre-training, Uni-Mol employs masked atom prediction, akin to BERT’s masked language modeling objective [13], corrupting 3D positional encodings with random noise at a 15% ratio. Additionally, the model is tasked with restoring the corrupted Euclidean distances between atoms and the coordinates for atoms.

Our codebase is developed atop the publicly accessible Uni-Mol repository,⁵ and their pre-trained checkpoint for molecular prediction serves as our model initialization.⁶ During fine-tuning, Uni-Mol generates 10 3D conformations for each molecule, supplemented with an additional 2D graph structure when 3D conformations cannot be produced. Hence, Uni-Mol samples from these 11 molecular representations for each molecule in every training epoch. For testing, we average the logits from all 11 representations to generate the final output logits. For implementation, we utilize the conformations prepared by the Uni-Mol repository.⁷

⁴Repository available at <https://github.com/tencent-ailab/grover>, and model can be downloaded at https://ai.tencent.com/ailab/ml/ml-data/grover-models/pretrain/grover_base.tar.gz.

⁵<https://github.com/dptech-corp/Uni-Mol/tree/main>.

⁶https://github.com/dptech-corp/Uni-Mol/releases/download/v0.1/mol_pre_no_h_220816.pt.

⁷The link is available in appendix A.

We configure the fine-tuning batch size at 128, the number of epochs at 100, and employ early stopping with a tolerance of 40 epochs. We use a linear learning rate scheduler with a 0.1 warm-up ratio and a peak learning rate of 5×10^{-5} . The model is trained with a dropout ratio of 0.1. Although the Uni-Mol repository provides a set of recommended hyperparameters, we observe no discernible improvement in model performance with these settings.

DNN The Deep Neural Network (DNN) serves as a simple, non-pre-trained baseline model designed to explore how heuristic descriptors like Morgan fingerprints [53] or RDKit features perform for molecular property prediction. For the descriptor, we adopt the approach of previous work [84, 86, 64] and extract 200-dimensional molecule-level features using RDKit for each molecule, which are then used as DNN input.⁸ The DNN consists of 8 fully-connected 128-dimensional hidden layers with GELU activation and an intervening dropout ratio of 0.1. We found no performance gain from deeper or wider DNNs and thus assume that our model is fully capable of harnessing the expressivity of RDKit features. The model is trained with a batch size of 256 and a constant learning rate of 2×10^{-4} for 400 epochs with an early stopping tolerance of 50 epochs.

C Uncertainty Quantification

Focal Loss First proposed in [47] Focal loss is designed to address the class imbalance issue for dense object detection in computer vision, where the number of negative samples (background) far exceeds the number of positive ones (objects). It is adopted to uncertainty estimation and model calibration later in [55]. The idea is to add a modulating factor to the standard cross-entropy loss to down-weight the contribution from easy examples and thus focus more on hard examples. In the binary classification case, it adds a modulating factor $|y_n - \hat{p}_n|^\gamma$ to the standard cross-entropy loss, where $y_n \in \{0, 1\}$ is the ground truth label, $\hat{p}_n \in (0, 1)$ is the predicted Sigmoid probability for the n -th example, and $\gamma \geq 0$ is a focusing parameter:

$$\mathcal{L}_{\text{focal}} = -\frac{1}{N} \sum_{n=1}^N [y_n(1 - \hat{p}_n)^\gamma \log \hat{p}_n + (1 - y_n)\hat{p}_n^\gamma \log(1 - \hat{p}_n)]. \quad (1)$$

The focusing parameter γ smoothly adjusts the rate at which easy examples are down-weighted. When $\gamma = 0$, focal loss is equivalent to cross-entropy loss. As γ is increased, the effect of the modulating factor is likewise increased. In our implementation, we take advantage of the realization in the `torchvision` library and use their default hyper-parameters for all experiments.⁹

Bayes by Backprop Bayes by Backprop (BBP) [6] is an algorithm for training Bayesian neural networks (BNNs), where weights are not point estimates but distributions. The idea is to replace the deterministic network weights with Gaussian a posteriori learned from the data, which allows quantifying the uncertainty in the predictions by assembling the predictions from random networks sampled from the posterior distribution of the weights:

$$\mathbf{w}^{\text{MAP}} = \arg \max_{\mathbf{w}} \log p(\mathbf{w}|\mathcal{D}) = \arg \max_{\mathbf{w}} (\log p(\mathcal{D}|\mathbf{w}) + \log p(\mathbf{w})), \quad (2)$$

where $p(\mathbf{w})$ is the prior distribution of the weights, which are also Gaussian in our realization.

However, the true posterior is generally intractable for neural networks and can only be approximated with variational inference $q(\mathbf{w}|\boldsymbol{\theta})$ [41], where $\boldsymbol{\theta}$ are variational parameters. In our case, the variational parameters consist of the mean and standard deviation of multi-variate Gaussian distribution $\boldsymbol{\theta} = \{\boldsymbol{\mu}, \boldsymbol{\rho}\}$. The learning then involves finding the $\boldsymbol{\theta}$ that minimizes the Kullback-Leibler (KL) divergence between the true posterior and the variational distribution. The loss can be written as

$$\mathcal{L} = \text{KL}[q(\mathbf{w}|\boldsymbol{\theta})||p(\mathbf{w})] - \mathbb{E}_{q(\mathbf{w}|\boldsymbol{\theta})}[\log p(\mathcal{D}|\mathbf{w})]. \quad (3)$$

For each training step i , we first draw a sample from a posteriori $\mathbf{w}_i \sim q(\mathbf{w}|\boldsymbol{\theta})$ and then compute the Monte Carlo estimation of the loss:

$$\mathcal{L}_i \approx \log q(\mathbf{w}_i|\boldsymbol{\theta}) - \log p(\mathbf{w}_i) - \log p(\mathcal{D}|\mathbf{w}_i). \quad (4)$$

⁸We use the “rdkit2dnormalized” descriptor in `DescriptorStorus`, available at <https://github.com/bp-kelley/descriptastorus>.

⁹https://pytorch.org/vision/main/generated/torchvision.ops.sigmoid_focal_loss.html.

During backpropagation, the gradient can be pushed through the sampling process with the reparameterization trick [41]. Specifically, we adopt the local reparameterization trick [40], which samples the pre-activation \mathbf{a}_i from the distribution $q(\mathbf{a}_i|\mathbf{x}_i)$ instead of the weights w_i from a distribution $q(\mathbf{w}_i|\boldsymbol{\theta})$ and computing the pre-activation as $\mathbf{a}_i = \mathbf{w}_i\mathbf{x}$. This has parameters that are deterministic functions of \mathbf{x} and $\boldsymbol{\theta}$, which reduces the variance of the gradient estimates and can improve the efficiency of the learning process. Additionally, we only apply BBP to the last layer of the model to reduce computational costs and implementation difficulty for large pre-trained backbone models. During the test, we sample 30 networks from the posterior distribution, generating 30 sets of prediction results, and computing the mean of the predictions as the final output.

SGLD Stochastic gradient Langevin dynamics (SGLD) [82] combines the efficiency of stochastic gradient descent (SGD) with Langevin diffusion which introduces the ability to estimate parameter a posteriori. The update rule for SGLD is given by:

$$\Delta\boldsymbol{\theta} = -\frac{\eta_t}{2}\nabla\mathcal{L}(\boldsymbol{\theta}) + \sqrt{\eta_t}\boldsymbol{\epsilon}, \quad (5)$$

where $\boldsymbol{\theta}$ is the network parameters, η_t is the learning rate at time t , and $\boldsymbol{\epsilon}_t$ is the standard Gaussian noise. With learning rate $\boldsymbol{\theta}$ or weight gradient $\nabla\mathcal{L}(\boldsymbol{\theta})$ decreasing to small values, the update rule can transit from network optimization to posterior estimation. After sufficient optimization, subsequent samples of parameters can be seen as drawing from the posterior distribution of the model parameters given the data.

In our implementation, we follow the previous implementation and use a constant learning rate.¹⁰ Similar to BBP, we only apply SGLD to the last layer of the model. We first train the model to the best and then continue training it for 30 epochs, resulting in 30 networks sampled from the Langevin dynamics. This generates 30 sets of prediction results during the test, and we compute the mean of the predictions as the final output.

MC Dropout Compared to other Bayesian networks, Monte-Carlo Dropout (MC Dropout) [18] is a simple and efficient for modeling the network uncertainty. Dropout [71] is proposed to prevent overfitting by randomly setting some neurons' outputs to zero during training. At test time, dropout is deactivated and the weights are scaled down by the dropout rate to simulate the presence of all neurons. In contrast, MC Dropout proposes to keep dropout active during testing and make predictions with dropout turned on. By running several (*e.g.*, 30 in experiments) forward passes with random dropout masks, we effectively obtain a Monte Carlo estimation of the predictive distribution.

SWAG Stochastic Weight Averaging-Gaussian (SWAG) [51] is an extension of the Stochastic Weight Averaging (SWA) method [35], a technique used for finding wider optima in the loss landscape, which leads to improved generalization. SWAG fits a Gaussian distribution with a low rank plus diagonal covariance derived from the SGD iterates to approximate the posterior distribution over neural network weights. In SWAG, the model keeps tracking the weights encountered during the last T steps of the stochastic gradient descent updates and computes the Gaussian mean and covariance:

$$\begin{aligned} \boldsymbol{\mu}_\theta &= \frac{1}{T} \sum_{t=1}^T \boldsymbol{\theta}_t; \\ \boldsymbol{\Sigma}_\theta &= \frac{1}{T} \sum_{t=1}^T (\boldsymbol{\theta}_t - \boldsymbol{\mu}_\theta)(\boldsymbol{\theta}_t - \boldsymbol{\mu}_\theta)^\top. \end{aligned} \quad (6)$$

However, such computation requires storing all the model weights in the last T steps, which is expensive for large models. To address this issue, Maddox et al. [51] propose to approximate the covariance matrix with a low-rank plus diagonal matrix, and compute the mean and covariance iteratively. Specifically, at update step $t \in \{1, \dots, T\}$,

$$\bar{\boldsymbol{\theta}}_t = \frac{t\bar{\boldsymbol{\theta}}_{t-1} + \boldsymbol{\theta}_t}{t+1}; \quad \bar{\boldsymbol{\theta}}_t^2 = \frac{t\bar{\boldsymbol{\theta}}_{t-1}^2 + \boldsymbol{\theta}_t^2}{t+1}; \quad \hat{D}_{:,t} = \boldsymbol{\theta}_t - \bar{\boldsymbol{\theta}}_t, \quad (7)$$

where $\bar{\boldsymbol{\theta}}_0$ is the best parameter weights found during training prior to the SWA session, $\bar{\boldsymbol{\theta}}_T^2 - \bar{\boldsymbol{\theta}}_0^2$ is the covariance diagonal, and $\frac{1}{T-1}\hat{D}\hat{D}^\top \in \mathbb{R}^{d,d}$ is the low-rank approximation of the covariance

¹⁰<https://github.com/JavierAntoran/Bayesian-Neural-Networks/>.

matrix with d being the parameter dimensionality. We can write the Gaussian weight posterior as

$$\boldsymbol{\theta}_{\text{SWAG}} \sim \mathcal{N}_{\text{SWAG}} \left(\bar{\boldsymbol{\theta}}_T, \frac{1}{2} \left(\bar{\boldsymbol{\theta}}^2_T - \bar{\boldsymbol{\theta}}^2_T + \frac{1}{T-1} \hat{D} \hat{D}^\top \right) \right). \quad (8)$$

Notice that \hat{D} has a different rank $K \leq T$ in [51], but we make $K = T < d$ for simplicity. Uncertainty in SWAG is estimated by drawing weight samples from $\mathcal{N}_{\text{SWAG}}$ and running these through the network. We set $T = 20$, and draw 30 samples during the test in our experiments.

Temperature Scaling Temperature scaling [60, 27] is a simple and effective post-hoc method for calibrating the confidence of a neural network. Post-hoc calibration methods calibrate the output probabilities of a pre-trained model without any retraining. The core idea behind temperature scaling is to add a learnable parameter h (the temperature) to adjust the output probability of the model. For a trained binary classification model, temperature scaling scales the logits z with

$$z' = \frac{z}{h} \quad (9)$$

before feeding z' into the Sigmoid function. The temperature h is learned by minimizing the negative log-likelihood of the training data with other network parameters frozen. For multi-task classification such as Tox21, we assign an individual temperature to each task.

Deep Ensembles Deep Ensembles [45] is a technique where multiple deep learning models are independently trained from different initializations, and their predictions are combined to make a final prediction. This approach exploits the idea that different models will make different types of errors, which can be reduced by averaging model predictions, leading to better overall performance and more robust uncertainty estimates. Formally, given M models in the ensemble, each with parameters $\boldsymbol{\theta}_i$, the ensemble prediction for an input data point \boldsymbol{x} is given by:

$$\hat{y} = \frac{1}{M} \sum_{m=1}^M f(\boldsymbol{x}; \boldsymbol{\theta}_m) \quad (10)$$

where $f(\boldsymbol{x}; \boldsymbol{\theta}_m)$ is the prediction of the m -th model. We set $M = 3$ for QM8, QM9 and MUV, and $M = 10$ for other datasets.

For regression tasks, the original implementation [45] aggregates the variances of different network predictions through parameterizing a Gaussian mixture model. But we take a simpler approach by computing the mean of the variances as the final output variance.

D Metrics

In this section, we elaborate on the metrics utilized in our research for both property prediction and uncertainty estimation.

D.1 Prediction Metrics

ROC-AUC The receiver operating characteristic area under the curve (ROC-AUC) is widely used for binary classification tasks. The ROC curve plots the true positive rate (TPR), or *recall*, against the false positive rate (FPR) at various decision thresholds $t \in (0, 1)$. Given a set of true positives (TP), true negatives (TN), false positives (FP), and false negatives (FN), the TPR and FPR are computed as $\text{TPR} = \frac{\text{TP}}{\text{TP} + \text{FN}}$ and $\text{FPR} = \frac{\text{FP}}{\text{FP} + \text{TN}}$ respectively. The AUC signifies the likelihood of a randomly selected positive instance being ranked above a randomly chosen negative instance. This integral under the ROC curve is calculated as

$$\text{ROC-AUC} = \int_0^1 \text{TPR}(t) \frac{d\text{FPR}(t)}{dt} dt \quad (11)$$

and can be approximated using numerical methods.¹¹

¹¹We use `scikit-learn`'s `roc_auc_score` function in our implementation.

RMSE For regression tasks, the root mean square error (RMSE) quantifies the average discrepancy between predicted ($\hat{y}_n \in \mathbb{R}$) and actual ($y_n \in \mathbb{R}$) values for N data points, given by:

$$\text{RMSE} = \sqrt{\frac{1}{N} \sum_{n=1}^N (\hat{y}_n - y_n)^2}. \quad (12)$$

MAE The mean absolute error (MAE) is another regression metric, measuring the average absolute deviation between predicted and actual values. It is calculated as:

$$\text{MAE} = \frac{1}{N} \sum_{i=1}^N |\hat{y}_n - y_n|. \quad (13)$$

D.2 Uncertainty Quantification Metrics

NLL Negative log-likelihood (NLL) quantifies the mean deviation between predicted and actual values in logarithmic space and is commonly used to evaluate UQ performance [18, 45, 21]. For binary classification with Sigmoid output activation, the NLL is given by:

$$\text{NLL} = -\frac{1}{N} \sum_{n=1}^N [y_n \log \hat{p}_n + (1 - y_n) \log(1 - \hat{p}_n)], \quad (14)$$

where $y_n \in \{0, 1\}$ is the true label and $\hat{p}_n \in (0, 1)$ is the predicted probability.

For regression, the Gaussian NLL is calculated as:

$$\text{NLL} = -\frac{1}{N} \sum_{n=1}^N \mathcal{N}(y_n; \hat{y}_n, \hat{\sigma}_n) = \frac{1}{N} \sum_{n=1}^N \frac{1}{2} \left[\log(2\pi\hat{\sigma}_n) + \frac{(y_n - \hat{y}_n)^2}{\hat{\sigma}_n} \right], \quad (15)$$

where $\hat{y}_n \in \mathbb{R}$ is the predicted mean and $\hat{\sigma}_n \in \mathbb{R}_+$ is the predicted variance.

Brier Score In classification, the Brier score (BS) is a proper scoring rule for measuring the accuracy of predicted probabilities. Similar to mean square error (MSE) in regression, it measures the mean squared difference between predicted probabilities and actual binary outcomes. For binary classification, the Brier score is calculated as

$$\text{Brier Score} = \frac{1}{N} \sum_{i=1}^N (\hat{p}_n - y_n)^2, \quad (16)$$

where $y_n \in \{0, 1\}$ and $\hat{p}_n \in (0, 1)$.

ECE Expected calibration error (ECE) measures the average difference between predicted probabilities and their corresponding empirical probabilities, whose calculation is detailed in section 3 and rewritten here specifically for the binary classification case.

ECE puts the predicted probabilities $\{\hat{p}_n\}_{n=1}^N$ into S (which is set to $S = 15$ in our experiments) equal-width bins $B_s = \{n \in \{1, \dots, N\} \mid \hat{p}_n \in (\rho_s, \rho_{s+1}]\}$ with $s \in \{1, \dots, S\}$ and $\rho_s = \frac{s}{S}$. Then ECE is calculated as

$$\text{ECE} = \sum_{s=1}^S \frac{|B_s|}{N} |\text{acc}(B_s) - \text{conf}(B_s)|; \quad (17)$$

$$\text{acc}(B_s) = \frac{1}{|B_s|} \sum_{n \in B_s} \mathbf{1}(|y_n - \hat{p}_n| < 0.5); \quad \text{conf}(B_s) = \frac{1}{|B_s|} \sum_{n \in B_s} \hat{p}_n,$$

where $\mathbf{1}(\cdot)$ is the indicator function. Notice that $|\cdot|$ represents the size of a set when its input is a set, and the absolute value when its input is a real number.

Regression CE Regression calibration is less studied than classification calibration, and regression calibration error (CE), proposed in [44], is adopted in only a few works such as [70, 37]. Similar to ECE, CE measures the average difference between the observed confidence level and the expected confidence level within each bin. Specifically, a confidence level of α is measured as the fraction of data points whose true value falls within the $\frac{1-\alpha}{2}$ th quantile and $(1 - \frac{\alpha}{2})$ th quantile of the predicted distribution. For example, 90% confidence level contains data points with true values falling within the 5%th quantile and 95%th quantile of the predicted distribution. With this established, we can calculate the confidence levels with the predicted quantile function, in our case, the cumulative distribution function (CDF) of the predicted Gaussian. Specifically,

$$\text{CE} = \frac{1}{S} \sum_{s=1}^S \left(\rho_s - \frac{1}{N} |\{n \in \{1, \dots, N\} \mid \Phi(y_n; \hat{y}_n, \hat{\sigma}_n) \leq \rho_s\}| \right)^2 \quad (18)$$

where $\rho_s = \frac{s}{S}$ is the expected quantile, Φ is the Gaussian CDF, $\hat{y}_n \in \mathbb{R}$ the predicted mean and $\hat{\sigma}_n \in \mathbb{R}_+$ the variance. $\hat{p}_s = \frac{1}{N} |\{n \in \{1, \dots, N\} \mid \Phi(y_n; \hat{y}_n, \hat{\sigma}_n) \leq \rho_s\}|$ is the empirical frequency of the predicted values falling into the ρ_s th quantile. This is slightly different from the confidence level-based calculation, where

$$\text{CE} = \frac{2}{S} \sum_{s=1}^{\frac{S}{2}} ((\rho_{S-s} - \rho_s) - (\hat{p}_{S-s} - \hat{p}_s))^2, \quad (19)$$

but it reveals the same trend. We use $S = 20$ in our experiments.

E Results

Tables 5–12 illustrate scores associated with each backbone-UQ pairing across classification datasets, while Tables 13–18 detail the scores regarding regression metrics. Scores are represented in a “mean (standard deviation)” structure, where both mean and standard deviation values are derived from 3 experiment runs conducted with random seeds 0, 1, and 2. As deep ensembles UQ method aggregates network predictions prior to metric calculation, standard deviation values are not generated and metrics are calculated only once.

Challenges are encountered during training on the notably imbalanced MUV dataset, depicted in Table 3. SGLD at times proves unsuccessful due to weak directional cues from the true labels, overwhelmed by the random noise embedded in the Langevin dynamics. Conversely, the application of Focal loss demonstrates effective performance on the MUV dataset, aligning with assertions in [47]. ECE also occasionally fails to compute on MUV as predicted probabilities \hat{p} are excessively minimal, leading to unpopulated bins and subsequent "division by zero" errors.

In terms of the majority of datasets, the performance trends closely adhere to our previous discussions. However, an anomaly is observed with the ClinTox dataset, where ChemBERTa produces anomalously high performance, deviating from prior findings [1, 90]. Conceptually, the ChemBERTa checkpoint we use is solely pre-trained on the masked language modeling (MLM) objective, which is unrelated to downstream tasks and should not include label information. Consequently, we hypothesize that the checkpoint may have undergone fine-tuning prior to upload, resulting in potential contamination.

Table 5: Test results on BACE in the format of “metric mean (standard deviation)”.

		ROC-AUC	ECE	NLL	BS
DNN-rdkit	Deterministic	0.8185 (0.0164)	0.2827 (0.0155)	0.8946 (0.0797)	0.2810 (0.0125)
	Temperature	0.8185 (0.0164)	0.2537 (0.0144)	0.7412 (0.0472)	0.2553 (0.0111)
	Focal Loss	0.8190 (0.0112)	0.2543 (0.0011)	0.6908 (0.0099)	0.2488 (0.0027)
	MC Dropout	0.8168 (0.0121)	0.2648 (0.0323)	0.7667 (0.0446)	0.2589 (0.0157)
	SWAG	0.8173 (0.0119)	0.2728 (0.0068)	0.8730 (0.0643)	0.2730 (0.0085)
	BBP	0.8288 (0.0039)	0.2711 (0.0193)	0.7943 (0.0235)	0.2535 (0.0075)
	SGLD	0.8181 (0.0160)	0.2713 (0.0024)	0.9023 (0.0416)	0.2734 (0.0073)
	Ensembles	0.8207 (-)	0.2550 (-)	0.7985 (-)	0.2557 (-)
ChemBERTa	Deterministic	0.7223 (0.0089)	0.2407 (0.0135)	0.7567 (0.0203)	0.2720 (0.0081)
	Temperature	0.7223 (0.0089)	0.1758 (0.0059)	0.6937 (0.0118)	0.2498 (0.0052)
	Focal Loss	0.6985 (0.0062)	0.2140 (0.0070)	0.7322 (0.0051)	0.2679 (0.0023)
	MC Dropout	0.7613 (0.0216)	0.2391 (0.0262)	0.7464 (0.0257)	0.2673 (0.0070)
	SWAG	0.7580 (0.0139)	0.2539 (0.0091)	0.7707 (0.0374)	0.2654 (0.0139)
	BBP	0.7372 (0.0233)	0.2767 (0.0032)	0.8325 (0.0190)	0.2878 (0.0046)
	SGLD	0.7775 (0.0205)	0.2492 (0.0217)	0.7922 (0.0283)	0.2588 (0.0069)
	Ensembles	0.7350 (-)	0.2352 (-)	0.7457 (-)	0.2683 (-)
GROVER	Deterministic	0.8308 (0.0012)	0.2304 (0.0658)	0.6921 (0.1114)	0.2342 (0.0386)
	Temperature	0.8305 (0.0017)	0.2083 (0.0521)	0.6251 (0.0671)	0.2184 (0.0283)
	Focal Loss	0.8509 (0.0072)	0.2334 (0.0302)	0.6397 (0.0300)	0.2281 (0.0141)
	MC Dropout	0.8278 (0.0011)	0.2366 (0.0629)	0.6899 (0.1094)	0.2368 (0.0394)
	SWAG	0.8604 (0.0048)	0.2239 (0.0016)	0.6656 (0.0169)	0.2148 (0.0030)
	BBP	0.8322 (0.0099)	0.2570 (0.0331)	0.7001 (0.0583)	0.2450 (0.0228)
	SGLD	0.8494 (0.0028)	0.2281 (0.0066)	0.6769 (0.0144)	0.2204 (0.0038)
	Ensembles	0.8388 (-)	0.2288 (-)	0.6571 (-)	0.2252 (-)
Uni-Mol	Deterministic	0.8080 (0.0266)	0.2419 (0.0409)	0.7928 (0.1639)	0.2517 (0.0335)
	Temperature	0.8087 (0.0277)	0.2125 (0.0259)	0.6782 (0.0662)	0.2352 (0.0212)
	Focal Loss	0.8208 (0.0259)	0.2445 (0.0287)	0.6721 (0.0482)	0.2406 (0.0198)
	MC Dropout	0.8268 (0.0269)	0.2483 (0.0333)	0.8065 (0.1383)	0.2512 (0.0331)
	SWAG	0.8193 (0.0106)	0.2677 (0.0075)	0.9415 (0.0623)	0.2625 (0.0058)
	BBP	0.8386 (0.0135)	0.2673 (0.0473)	0.8158 (0.1584)	0.2588 (0.0375)
	SGLD	0.8699 (0.0118)	0.2437 (0.0131)	0.7354 (0.0502)	0.2244 (0.0150)
	Ensembles	0.8505 (-)	0.2176 (-)	0.6301 (-)	0.2184 (-)

Table 6: Test results on BBBP in the format of “metric mean (standard deviation)”.

		ROC-AUC	ECE	NLL	BS
DNN-rdkit	Deterministic	0.6721 (0.0129)	0.3292 (0.0517)	3.8147 (4.0782)	0.3423 (0.0378)
	Temperature	0.6719 (0.0129)	0.2890 (0.0742)	2.1338 (1.8963)	0.3186 (0.0489)
	Focal Loss	0.6693 (0.0047)	0.1689 (0.1056)	0.8925 (0.3424)	0.2623 (0.0470)
	MC Dropout	0.6669 (0.0151)	0.3287 (0.0402)	2.1699 (1.7478)	0.3391 (0.0296)
	SWAG	0.6777 (0.0136)	0.3020 (0.0694)	4.8415 (5.5407)	0.3268 (0.0465)
	BBP	0.6856 (0.0075)	0.3392 (0.0506)	1.8126 (0.6030)	0.3463 (0.0357)
	SGLD	0.6922 (0.0125)	0.3134 (0.0487)	1.7569 (1.0592)	0.3247 (0.0396)
	Ensembles	0.7018 (-)	0.2615 (-)	0.9043 (-)	0.2938 (-)
ChemBERTa	Deterministic	0.7407 (0.0101)	0.2259 (0.0206)	1.0306 (0.1002)	0.2559 (0.0090)
	Temperature	0.7407 (0.0101)	0.2107 (0.0196)	0.8539 (0.0266)	0.2453 (0.0064)
	Focal Loss	0.7410 (0.0122)	0.1639 (0.0118)	0.6995 (0.0246)	0.2313 (0.0087)
	MC Dropout	0.7451 (0.0067)	0.2082 (0.0035)	0.8814 (0.0292)	0.2418 (0.0032)
	SWAG	0.7408 (0.0112)	0.2373 (0.0202)	1.1435 (0.0810)	0.2629 (0.0109)
	BBP	0.7245 (0.0112)	0.2415 (0.0293)	0.9653 (0.1062)	0.2652 (0.0120)
	SGLD	0.7359 (0.0104)	0.2398 (0.0256)	1.0692 (0.1940)	0.2580 (0.0056)
	Ensembles	0.7399 (-)	0.2290 (-)	0.9672 (-)	0.2506 (-)
GROVER	Deterministic	0.7075 (0.0061)	0.2902 (0.0111)	0.9457 (0.0234)	0.2998 (0.0060)
	Temperature	0.7072 (0.0059)	0.2685 (0.0147)	0.8607 (0.0258)	0.2865 (0.0069)
	Focal Loss	0.7146 (0.0059)	0.1340 (0.0177)	0.6505 (0.0070)	0.2284 (0.0040)
	MC Dropout	0.7066 (0.0071)	0.2901 (0.0147)	0.9267 (0.0285)	0.2996 (0.0071)
	SWAG	0.7160 (0.0032)	0.3314 (0.0032)	1.1105 (0.0142)	0.3251 (0.0025)
	BBP	0.6968 (0.0152)	0.2735 (0.0209)	0.9146 (0.0326)	0.2986 (0.0055)
	SGLD	0.7266 (0.0037)	0.3127 (0.0065)	1.0187 (0.0202)	0.3149 (0.0019)
	Ensembles	0.7083 (-)	0.2890 (-)	0.9338 (-)	0.3029 (-)
Uni-Mol	Deterministic	0.7103 (0.0075)	0.3311 (0.0506)	1.4209 (0.3000)	0.3354 (0.0397)
	Temperature	0.7093 (0.0083)	0.2922 (0.0418)	1.0023 (0.1064)	0.3084 (0.0315)
	Focal Loss	0.7102 (0.0045)	0.2031 (0.0816)	0.7646 (0.0923)	0.2632 (0.0275)
	MC Dropout	0.7029 (0.0142)	0.3328 (0.0483)	1.4086 (0.2828)	0.3382 (0.0372)
	SWAG	0.7247 (0.0062)	0.3547 (0.0136)	1.8530 (0.0824)	0.3456 (0.0078)
	BBP	0.6902 (0.0286)	0.3420 (0.0318)	1.3548 (0.0713)	0.3463 (0.0275)
	SGLD	0.7147 (0.0118)	0.3336 (0.0127)	1.4174 (0.0475)	0.3359 (0.0059)
	Ensembles	0.7253 (-)	0.3035 (-)	1.0889 (-)	0.3035 (-)

Table 7: Test results on ClinTox in the format of “metric mean (standard deviation)”.

		ROC-AUC	ECE	NLL	BS
DNN-rdkit	Deterministic	0.8301 (0.0226)	0.0637 (0.0126)	0.2719 (0.0481)	0.0597 (0.0052)
	Temperature	0.8300 (0.0224)	0.0547 (0.0109)	0.2371 (0.0059)	0.0572 (0.0039)
	Focal Loss	0.8507 (0.0165)	0.0812 (0.0368)	0.2284 (0.0305)	0.0639 (0.0114)
	MC Dropout	0.8194 (0.0217)	0.0445 (0.0055)	0.2149 (0.0307)	0.0534 (0.0005)
	SWAG	0.8290 (0.0163)	0.0590 (0.0117)	0.2964 (0.0617)	0.0591 (0.0054)
	BBP	0.7541 (0.0102)	0.0574 (0.0121)	0.2439 (0.0276)	0.0609 (0.0046)
	SGLD	0.8335 (0.0109)	0.0567 (0.0125)	0.2769 (0.0452)	0.0553 (0.0063)
	Ensembles	0.8154 (-)	0.0283 (-)	0.1860 (-)	0.0484 (-)
ChemBERTa	Deterministic	0.9856 (0.0028)	0.0215 (0.0035)	0.1206 (0.0318)	0.0225 (0.0016)
	Temperature	0.9856 (0.0028)	0.0199 (0.0026)	0.0964 (0.0147)	0.0222 (0.0013)
	Focal Loss	0.9832 (0.0027)	0.0897 (0.0378)	0.1367 (0.0350)	0.0273 (0.0045)
	MC Dropout	0.9848 (0.0021)	0.0212 (0.0019)	0.1083 (0.0247)	0.0213 (0.0021)
	SWAG	0.9850 (0.0031)	0.0222 (0.0025)	0.1327 (0.0317)	0.0232 (0.0010)
	BBP	0.9816 (0.0079)	0.0325 (0.0212)	0.0972 (0.0156)	0.0226 (0.0024)
	SGLD	0.9869 (0.0012)	0.0183 (0.0006)	0.0893 (0.0050)	0.0214 (0.0005)
	Ensembles	0.9812 (-)	0.0157 (-)	0.0810 (-)	0.0208 (-)
GROVER	Deterministic	0.9398 (0.0152)	0.0635 (0.0114)	0.1471 (0.0106)	0.0367 (0.0031)
	Temperature	0.9409 (0.0130)	0.0449 (0.0055)	0.1260 (0.0045)	0.0333 (0.0034)
	Focal Loss	0.9377 (0.0042)	0.2158 (0.0034)	0.2963 (0.0018)	0.0731 (0.0011)
	MC Dropout	0.9347 (0.0152)	0.0706 (0.0122)	0.1475 (0.0121)	0.0366 (0.0036)
	SWAG	0.9623 (0.0060)	0.0460 (0.0117)	0.1119 (0.0046)	0.0280 (0.0022)
	BBP	0.9085 (0.0109)	0.0940 (0.0104)	0.1976 (0.0136)	0.0488 (0.0033)
	SGLD	0.9507 (0.0058)	0.0595 (0.0065)	0.1287 (0.0063)	0.0306 (0.0011)
	Ensembles	0.9429 (-)	0.0743 (-)	0.1453 (-)	0.0344 (-)
Uni-Mol	Deterministic	0.8814 (0.0379)	0.0522 (0.0120)	0.1822 (0.0381)	0.0484 (0.0124)
	Temperature	0.8830 (0.0375)	0.0417 (0.0158)	0.1754 (0.0358)	0.0477 (0.0121)
	Focal Loss	0.8836 (0.0202)	0.1651 (0.0556)	0.2972 (0.0587)	0.0827 (0.0207)
	MC Dropout	0.8745 (0.0438)	0.0560 (0.0131)	0.1889 (0.0406)	0.0521 (0.0138)
	SWAG	0.9055 (0.0027)	0.0311 (0.0034)	0.1450 (0.0035)	0.0337 (0.0009)
	BBP	0.9257 (0.0287)	0.0379 (0.0026)	0.1468 (0.0047)	0.0398 (0.0032)
	SGLD	0.8598 (0.0209)	0.0327 (0.0029)	0.1619 (0.0059)	0.0389 (0.0014)
	Ensembles	0.9088 (-)	0.0389 (-)	0.1476 (-)	0.0386 (-)

Table 8: Test results on Tox21 in the format of “metric mean (standard deviation)”.

		ROC-AUC	ECE	NLL	BS
DNN-rdkit	Deterministic	0.7386 (0.0061)	0.0417 (0.0028)	0.2771 (0.0024)	0.0779 (0.0013)
	Temperature	0.7386 (0.0061)	0.0342 (0.0027)	0.2723 (0.0028)	0.0773 (0.0013)
	Focal Loss	0.7374 (0.0038)	0.1058 (0.0060)	0.3161 (0.0078)	0.0871 (0.0024)
	MC Dropout	0.7376 (0.0039)	0.0356 (0.0016)	0.2727 (0.0016)	0.0763 (0.0013)
	SWAG	0.7364 (0.0045)	0.0438 (0.0010)	0.2793 (0.0037)	0.0790 (0.0017)
	BBP	0.7243 (0.0036)	0.0422 (0.0019)	0.2847 (0.0010)	0.0814 (0.0002)
	SGLD	0.7257 (0.0018)	0.1192 (0.0332)	0.3455 (0.0315)	0.0978 (0.0100)
	Ensembles	0.7540 (-)	0.0344 (-)	0.2648 (-)	0.0746 (-)
ChemBERTa	Deterministic	0.7542 (0.0009)	0.0571 (0.0020)	0.2962 (0.0067)	0.0812 (0.0009)
	Temperature	0.7542 (0.0009)	0.0424 (0.0040)	0.2744 (0.0027)	0.0792 (0.0011)
	Focal Loss	0.7523 (0.0022)	0.0969 (0.0012)	0.3052 (0.0018)	0.0845 (0.0004)
	MC Dropout	0.7641 (0.0032)	0.0423 (0.0023)	0.2697 (0.0032)	0.0744 (0.0005)
	SWAG	0.7538 (0.0021)	0.0592 (0.0022)	0.3008 (0.0079)	0.0818 (0.0011)
	BBP	0.7433 (0.0055)	0.0459 (0.0028)	0.2765 (0.0035)	0.0780 (0.0014)
	SGLD	0.7475 (0.0036)	0.0504 (0.0038)	0.2784 (0.0030)	0.0795 (0.0014)
	Ensembles	0.7681 (-)	0.0440 (-)	0.2679 (-)	0.0750 (-)
GROVER	Deterministic	0.7808 (0.0017)	0.0358 (0.0038)	0.2473 (0.0022)	0.0694 (0.0005)
	Temperature	0.7810 (0.0016)	0.0291 (0.0016)	0.2439 (0.0008)	0.0686 (0.0003)
	Focal Loss	0.7779 (0.0028)	0.1148 (0.0102)	0.3052 (0.0094)	0.0811 (0.0028)
	MC Dropout	0.7817 (0.0018)	0.0346 (0.0015)	0.2455 (0.0016)	0.0689 (0.0005)
	SWAG	0.7837 (0.0017)	0.0359 (0.0009)	0.2482 (0.0009)	0.0689 (0.0001)
	BBP	0.7697 (0.0031)	0.0438 (0.0017)	0.2552 (0.0016)	0.0711 (0.0003)
	SGLD	0.7635 (0.0009)	0.0402 (0.0024)	0.2558 (0.0010)	0.0716 (0.0002)
	Ensembles	0.7876 (-)	0.0316 (-)	0.2411 (-)	0.0675 (-)
Uni-Mol	Deterministic	0.7895 (0.0017)	0.0454 (0.0056)	0.2601 (0.0072)	0.0716 (0.0022)
	Temperature	0.7896 (0.0016)	0.0346 (0.0027)	0.2483 (0.0035)	0.0704 (0.0014)
	Focal Loss	0.7904 (0.0040)	0.0972 (0.0045)	0.2899 (0.0009)	0.0785 (0.0001)
	MC Dropout	0.7891 (0.0021)	0.0480 (0.0066)	0.2628 (0.0065)	0.0726 (0.0021)
	SWAG	0.7842 (0.0048)	0.0593 (0.0025)	0.2994 (0.0054)	0.0728 (0.0012)
	BBP	0.7932 (0.0043)	0.0396 (0.0048)	0.2520 (0.0039)	0.0703 (0.0010)
	SGLD	0.7887 (0.0059)	0.0433 (0.0023)	0.2569 (0.0055)	0.0684 (0.0014)
	Ensembles	0.8052 (-)	0.0332 (-)	0.2389 (-)	0.0662 (-)

Table 9: Test results on ToxCast in the format of “metric mean (standard deviation)”.

		ROC-AUC	ECE	NLL	BS
DNN-rdkit	Deterministic	0.6222 (0.0042)	0.1168 (0.0096)	0.4436 (0.0146)	0.1397 (0.0021)
	Temperature	0.6220 (0.0046)	0.1114 (0.0050)	0.4882 (0.0170)	0.1398 (0.0015)
	Focal Loss	0.6289 (0.0077)	0.1264 (0.0034)	0.4389 (0.0084)	0.1396 (0.0024)
	MC Dropout	0.6248 (0.0030)	0.1093 (0.0075)	0.4319 (0.0096)	0.1358 (0.0015)
	SWAG	0.6207 (0.0073)	0.1175 (0.0098)	0.4440 (0.0150)	0.1400 (0.0023)
	BBP	0.6020 (0.0028)	0.1443 (0.0060)	0.4673 (0.0059)	0.1510 (0.0020)
	SGLD	0.5319 (0.0040)	0.3054 (0.0034)	0.6685 (0.0035)	0.2378 (0.0017)
	Ensembles	0.6486 (-)	0.0900 (-)	0.4008 (-)	0.1292 (-)
ChemBERTa	Deterministic	0.6554 (0.0037)	0.1209 (0.0026)	0.4313 (0.0054)	0.1330 (0.0008)
	Temperature	0.6540 (0.0042)	0.1067 (0.0019)	0.4817 (0.0261)	0.1313 (0.0004)
	Focal Loss	0.6442 (0.0170)	0.1197 (0.0037)	0.4243 (0.0153)	0.1346 (0.0051)
	MC Dropout	0.6624 (0.0024)	0.1069 (0.0036)	0.4070 (0.0052)	0.1276 (0.0015)
	SWAG	0.6556 (0.0033)	0.1202 (0.0036)	0.4305 (0.0064)	0.1327 (0.0010)
	BBP	0.5814 (0.0075)	0.1276 (0.0015)	0.4545 (0.0011)	0.1469 (0.0003)
	SGLD	0.5436 (0.0056)	0.2238 (0.0019)	0.5602 (0.0022)	0.1881 (0.0011)
	Ensembles	0.6733 (-)	0.1037 (-)	0.3986 (-)	0.1258 (-)
GROVER	Deterministic	0.6587 (0.0018)	0.1043 (0.0006)	0.4091 (0.0023)	0.1298 (0.0004)
	Temperature	0.6496 (0.0023)	0.1424 (0.0026)	0.4612 (0.0045)	0.1424 (0.0013)
	Focal Loss	0.6359 (0.0026)	0.1221 (0.0005)	0.4365 (0.0012)	0.1383 (0.0004)
	MC Dropout	0.6615 (0.0014)	0.1009 (0.0010)	0.4042 (0.0022)	0.1288 (0.0004)
	SWAG	0.6603 (0.0020)	0.1060 (0.0007)	0.4114 (0.0015)	0.1301 (0.0001)
	BBP	0.5995 (0.0026)	0.1731 (0.0041)	0.5090 (0.0040)	0.1660 (0.0015)
	SGLD	0.5542 (0.0069)	0.2712 (0.0008)	0.6194 (0.0006)	0.2139 (0.0003)
	Ensembles	0.6646 (-)	0.1034 (-)	0.4061 (-)	0.1290 (-)
Uni-Mol	Deterministic	0.6734 (0.0101)	0.1020 (0.0023)	0.3983 (0.0075)	0.1274 (0.0025)
	Temperature	0.7028 (0.0101)	0.1456 (0.0045)	0.4566 (0.0104)	0.1355 (0.0029)
	Focal Loss	0.6934 (0.0035)	0.1227 (0.0011)	0.4079 (0.0016)	0.1284 (0.0003)
	MC Dropout	0.6833 (0.0117)	0.1074 (0.0090)	0.4015 (0.0112)	0.1274 (0.0025)
	SWAG	0.6870 (0.0075)	0.1085 (0.0034)	0.4005 (0.0055)	0.1271 (0.0019)
	BBP	0.6273 (0.0066)	0.1296 (0.0065)	0.4522 (0.0068)	0.1456 (0.0021)
	SGLD	0.5700 (0.0005)	0.1953 (0.0033)	0.5207 (0.0029)	0.1717 (0.0012)
	Ensembles	0.6841 (-)	0.0953 (-)	0.3877 (-)	0.1247 (-)

Table 10: Test results on SIDER in the format of “metric mean (standard deviation)”.

		ROC-AUC	ECE	NLL	BS
DNN-rdkit	Deterministic	0.5981 (0.0152)	0.1188 (0.0344)	0.5462 (0.0469)	0.1760 (0.0124)
	Temperature	0.5981 (0.0152)	0.1033 (0.0271)	0.5186 (0.0270)	0.1709 (0.0094)
	Focal Loss	0.5864 (0.0071)	0.1663 (0.0217)	0.5605 (0.0193)	0.1893 (0.0075)
	MC Dropout	0.5977 (0.0164)	0.1071 (0.0271)	0.5245 (0.0304)	0.1705 (0.0084)
	SWAG	0.5988 (0.0210)	0.1206 (0.0333)	0.5477 (0.0491)	0.1764 (0.0125)
	BBP	0.5738 (0.0272)	0.1215 (0.0046)	0.5241 (0.0077)	0.1733 (0.0027)
	SGLD	0.5895 (0.0087)	0.1559 (0.0119)	0.5653 (0.0119)	0.1900 (0.0051)
	Ensembles	0.6158 (-)	0.0954 (-)	0.4950 (-)	0.1631 (-)
ChemBERTa	Deterministic	0.6146 (0.0078)	0.1483 (0.0102)	0.5740 (0.0217)	0.1804 (0.0055)
	Temperature	0.6146 (0.0078)	0.1275 (0.0104)	0.5256 (0.0138)	0.1721 (0.0043)
	Focal Loss	0.6119 (0.0105)	0.1498 (0.0136)	0.5346 (0.0129)	0.1777 (0.0046)
	MC Dropout	0.6166 (0.0022)	0.1136 (0.0143)	0.5191 (0.0131)	0.1672 (0.0037)
	SWAG	0.6149 (0.0095)	0.1527 (0.0090)	0.5836 (0.0230)	0.1825 (0.0056)
	BBP	0.6067 (0.0108)	0.1184 (0.0018)	0.5127 (0.0043)	0.1686 (0.0013)
	SGLD	0.6127 (0.0110)	0.1299 (0.0118)	0.5255 (0.0157)	0.1725 (0.0053)
	Ensembles	0.6193 (-)	0.1305 (-)	0.5396 (-)	0.1718 (-)
GROVER	Deterministic	0.6213 (0.0027)	0.1034 (0.0061)	0.5023 (0.0071)	0.1637 (0.0021)
	Temperature	0.6209 (0.0030)	0.0939 (0.0040)	0.4935 (0.0046)	0.1618 (0.0018)
	Focal Loss	0.6059 (0.0165)	0.1817 (0.0019)	0.5666 (0.0027)	0.1903 (0.0011)
	MC Dropout	0.6248 (0.0060)	0.0969 (0.0035)	0.4942 (0.0057)	0.1616 (0.0018)
	SWAG	0.6133 (0.0024)	0.1183 (0.0016)	0.5280 (0.0066)	0.1702 (0.0019)
	BBP	0.5926 (0.0052)	0.1347 (0.0014)	0.5367 (0.0023)	0.1762 (0.0009)
	SGLD	0.5989 (0.0129)	0.1012 (0.0040)	0.5017 (0.0051)	0.1637 (0.0019)
	Ensembles	0.6237 (-)	0.0878 (-)	0.4917 (-)	0.1604 (-)
Uni-Mol	Deterministic	0.6214 (0.0073)	0.1054 (0.0130)	0.5047 (0.0184)	0.1661 (0.0065)
	Temperature	0.6210 (0.0075)	0.0950 (0.0074)	0.4937 (0.0101)	0.1625 (0.0040)
	Focal Loss	0.6200 (0.0118)	0.1660 (0.0096)	0.5471 (0.0090)	0.1834 (0.0038)
	MC Dropout	0.6125 (0.0060)	0.1269 (0.0178)	0.5324 (0.0270)	0.1739 (0.0071)
	SWAG	0.6246 (0.0090)	0.1327 (0.0084)	0.5397 (0.0125)	0.1753 (0.0033)
	BBP	0.6301 (0.0260)	0.0991 (0.0130)	0.4928 (0.0119)	0.1612 (0.0049)
	SGLD	0.6323 (0.0108)	0.1286 (0.0093)	0.5408 (0.0137)	0.1725 (0.0030)
	Ensembles	0.6378 (-)	0.0872 (-)	0.4836 (-)	0.1585 (-)

Table 11: Test results on HIV in the format of “metric mean (standard deviation)”.

		ROC-AUC	ECE	NLL	BS
DNN-rdkit	Deterministic	0.7345 (0.0065)	0.0077 (0.0010)	0.1236 (0.0016)	0.0276 (0.0006)
	Temperature	0.7345 (0.0065)	0.0136 (0.0005)	0.1277 (0.0021)	0.0277 (0.0007)
	Focal Loss	0.7338 (0.0078)	0.1205 (0.0179)	0.2059 (0.0179)	0.0429 (0.0042)
	MC Dropout	0.7365 (0.0088)	0.0066 (0.0010)	0.1219 (0.0016)	0.0270 (0.0004)
	SWAG	0.7439 (0.0014)	0.0105 (0.0025)	0.1240 (0.0013)	0.0279 (0.0005)
	BBP	0.7541 (0.0120)	0.0181 (0.0065)	0.1235 (0.0036)	0.0277 (0.0011)
	SGLD	0.7414 (0.0019)	0.0160 (0.0048)	0.1313 (0.0061)	0.0281 (0.0007)
	Ensembles	0.7613 (-)	0.0074 (-)	0.1160 (-)	0.0260 (-)
ChemBERTa	Deterministic	0.7681 (0.0061)	0.0214 (0.0033)	0.1247 (0.0058)	0.0292 (0.0019)
	Temperature	0.7681 (0.0061)	0.0221 (0.0039)	0.1259 (0.0067)	0.0289 (0.0018)
	Focal Loss	0.7509 (0.0106)	0.0651 (0.0351)	0.1599 (0.0205)	0.0343 (0.0025)
	MC Dropout	0.7717 (0.0042)	0.0079 (0.0014)	0.1105 (0.0011)	0.0247 (0.0005)
	SWAG	0.7474 (0.0123)	0.0263 (0.0045)	0.1384 (0.0063)	0.0319 (0.0017)
	BBP	0.7672 (0.0031)	0.0217 (0.0043)	0.1241 (0.0071)	0.0289 (0.0027)
	SGLD	0.7224 (0.0095)	0.0374 (0.0011)	0.1602 (0.0106)	0.0376 (0.0002)
	Ensembles	0.7885 (-)	0.0205 (-)	0.1161 (-)	0.0267 (-)
GROVER	Deterministic	0.7979 (0.0045)	0.0078 (0.0032)	0.1133 (0.0019)	0.0263 (0.0005)
	Temperature	0.7977 (0.0046)	0.0120 (0.0011)	0.1154 (0.0022)	0.0265 (0.0004)
	Focal Loss	0.7746 (0.0113)	0.1286 (0.0223)	0.2156 (0.0259)	0.0444 (0.0066)
	MC Dropout	0.8002 (0.0018)	0.0077 (0.0028)	0.1126 (0.0006)	0.0261 (0.0001)
	SWAG	0.8021 (0.0033)	0.0090 (0.0019)	0.1118 (0.0018)	0.0258 (0.0005)
	BBP	0.7928 (0.0116)	0.0162 (0.0062)	0.1151 (0.0034)	0.0258 (0.0002)
	SGLD	0.7420 (0.0131)	0.0200 (0.0012)	0.1231 (0.0001)	0.0272 (0.0000)
	Ensembles	0.8103 (-)	0.0035 (-)	0.1081 (-)	0.0251 (-)
Uni-Mol	Deterministic	0.7913 (0.0042)	0.0189 (0.0063)	0.1335 (0.0225)	0.0273 (0.0014)
	Temperature	0.7915 (0.0041)	0.0151 (0.0017)	0.1190 (0.0040)	0.0269 (0.0009)
	Focal Loss	0.7785 (0.0073)	0.0713 (0.0251)	0.1561 (0.0205)	0.0316 (0.0032)
	MC Dropout	0.7858 (0.0044)	0.0229 (0.0091)	0.1557 (0.0339)	0.0294 (0.0033)
	SWAG	0.7786 (0.0061)	0.0264 (0.0015)	0.1676 (0.0160)	0.0286 (0.0011)
	BBP	0.7781 (0.0128)	0.0191 (0.0071)	0.1428 (0.0327)	0.0284 (0.0016)
	SGLD	0.7777 (0.0121)	0.0205 (0.0006)	0.1373 (0.0087)	0.0263 (0.0002)
	Ensembles	0.8020 (-)	0.0181 (-)	0.1181 (-)	0.0265 (-)

Table 12: Test results on MUV in the format of “metric mean (standard deviation)”.

		ROC-AUC	ECE	NLL	BS
DNN-rdkit	Deterministic	0.6029 (0.0576)	0.0015 (0.0003)	0.0326 (0.0196)	0.0026 (0.0001)
	Temperature	0.6059 (0.0538)	- (-)	0.0321 (0.0145)	0.0027 (0.0003)
	Focal Loss	0.6261 (0.0322)	0.0780 (0.0033)	0.0720 (0.0262)	0.0076 (0.0032)
	MC Dropout	0.6282 (0.0530)	0.0015 (0.0003)	0.0256 (0.0114)	0.0025 (0.0000)
	SWAG	0.5830 (0.0392)	0.0025 (0.0006)	0.0393 (0.0254)	0.0027 (0.0001)
	BBP	0.5974 (0.0287)	- (-)	0.0251 (0.0068)	0.0027 (0.0001)
	SGLD	0.4955 (0.0509)	0.2380 (0.0156)	0.2798 (0.0201)	0.0610 (0.0071)
	Ensembles	0.6736 (-)	0.0013 (-)	0.0175 (-)	0.0025 (-)
ChemBERTa	Deterministic	0.6695 (0.0343)	0.0030 (0.0001)	0.0241 (0.0011)	0.0029 (0.0000)
	Temperature	0.6695 (0.0343)	0.0026 (0.0003)	0.0196 (0.0010)	0.0029 (0.0000)
	Focal Loss	0.7150 (0.0038)	0.0208 (0.0119)	0.0333 (0.0100)	0.0040 (0.0007)
	MC Dropout	0.7168 (0.0100)	0.0026 (0.0003)	0.0230 (0.0027)	0.0026 (0.0001)
	SWAG	0.6672 (0.0342)	0.0031 (0.0000)	0.0261 (0.0015)	0.0029 (0.0000)
	BBP	0.5970 (0.0622)	0.0026 (0.0010)	0.0198 (0.0018)	0.0030 (0.0004)
	SGLD	0.5030 (0.0346)	0.0074 (0.0003)	0.0217 (0.0002)	0.0026 (0.0000)
	Ensembles	0.7224 (-)	0.0025 (-)	0.0197 (-)	0.0027 (-)
GROVER	Deterministic	0.7157 (0.0330)	0.0016 (0.0004)	0.0169 (0.0004)	0.0025 (0.0000)
	Temperature	0.7155 (0.0331)	0.0014 (0.0001)	0.0187 (0.0004)	0.0025 (0.0000)
	Focal Loss	0.6825 (0.0127)	0.0869 (0.0033)	0.0995 (0.0036)	0.0101 (0.0006)
	MC Dropout	0.7163 (0.0363)	0.0016 (0.0004)	0.0170 (0.0004)	0.0025 (0.0000)
	SWAG	0.7281 (0.0226)	0.0014 (0.0003)	0.0162 (0.0002)	0.0025 (0.0000)
	BBP	0.7490 (0.0068)	0.0052 (0.0015)	0.0192 (0.0011)	0.0025 (0.0000)
	SGLD	0.5532 (0.0255)	0.0375 (0.0009)	0.0488 (0.0008)	0.0039 (0.0001)
	Ensembles	0.7268 (-)	0.0014 (-)	0.0166 (-)	0.0025 (-)
Uni-Mol	Deterministic	0.7718 (0.0200)	0.0024 (0.0002)	0.0225 (0.0027)	0.0025 (0.0000)
	Temperature	0.7625 (0.0098)	0.0017 (0.0000)	0.0233 (0.0039)	0.0025 (0.0001)
	Focal Loss	0.8239 (0.0140)	0.0250 (0.0126)	0.0354 (0.0116)	0.0036 (0.0006)
	MC Dropout	0.7781 (0.0201)	0.0026 (0.0001)	0.0253 (0.0017)	0.0025 (0.0000)
	SWAG	0.7429 (0.0442)	0.0028 (0.0001)	0.0276 (0.0016)	0.0027 (0.0001)
	BBP	0.7394 (0.0140)	0.0016 (0.0002)	0.0169 (0.0002)	0.0025 (0.0000)
	SGLD	0.5901 (0.0200)	0.0014 (0.0000)	0.0178 (0.0000)	0.0025 (0.0000)
	Ensembles	0.7904 (-)	0.0023 (-)	0.0195 (-)	0.0025 (-)

Table 13: Test results on ESOL in the format of “metric mean (standard deviation)”.

		RMSE	MAE	NLL	CE
DNN-rdkit	Deterministic	0.9048 (0.0289)	0.6747 (0.0059)	1.0033 (0.3765)	0.0465 (0.0052)
	MC Dropout	0.9129 (0.0212)	0.6853 (0.0049)	1.0246 (0.3698)	0.0495 (0.0051)
	SWAG	0.9165 (0.0244)	0.6827 (0.0074)	0.9461 (0.3428)	0.0459 (0.0048)
	BBP	0.9557 (0.0298)	0.7070 (0.0237)	0.4306 (0.0325)	0.0325 (0.0038)
	SGLD	0.9630 (0.0425)	0.7175 (0.0302)	0.5101 (0.0380)	0.0162 (0.0017)
	Ensembles	0.8690 (-)	0.6455 (-)	0.5674 (-)	0.0453 (-)
ChemBERTa	Deterministic	1.0044 (0.0358)	0.7989 (0.0216)	2.2803 (0.1218)	0.0500 (0.0007)
	MC Dropout	0.9497 (0.0271)	0.7620 (0.0176)	1.4258 (0.1905)	0.0481 (0.0023)
	SWAG	0.9966 (0.0334)	0.7940 (0.0206)	2.5815 (0.2470)	0.0513 (0.0013)
	BBP	1.0125 (0.0113)	0.8139 (0.0110)	0.5990 (0.0499)	0.0337 (0.0013)
	SGLD	0.9978 (0.0340)	0.8083 (0.0225)	1.2727 (0.0711)	0.0464 (0.0013)
	Ensembles	0.9752 (-)	0.7763 (-)	1.4981 (-)	0.0470 (-)
GROVER	Deterministic	0.9355 (0.0252)	0.7396 (0.0193)	0.9888 (0.0395)	0.0451 (0.0006)
	MC Dropout	0.9437 (0.0246)	0.7491 (0.0216)	1.0065 (0.0351)	0.0449 (0.0007)
	SWAG	0.9443 (0.0219)	0.7420 (0.0189)	1.2996 (0.1883)	0.0470 (0.0011)
	BBP	0.9892 (0.0430)	0.7821 (0.0327)	0.5470 (0.0378)	0.0153 (0.0028)
	SGLD	0.9955 (0.0104)	0.7942 (0.0153)	0.4786 (0.0140)	0.0243 (0.0008)
	Ensembles	0.9110 (-)	0.7209 (-)	0.5854 (-)	0.0394 (-)
Uni-Mol	Deterministic	0.8530 (0.0224)	0.6809 (0.0164)	1.0739 (0.1136)	0.0527 (0.0004)
	MC Dropout	0.8367 (0.0237)	0.6648 (0.0209)	1.1098 (0.2625)	0.0527 (0.0012)
	SWAG	0.8644 (0.0097)	0.6950 (0.0042)	1.3868 (0.1522)	0.0540 (0.0003)
	BBP	0.8441 (0.0332)	0.6719 (0.0279)	0.3151 (0.0292)	0.0329 (0.0015)
	SGLD	0.8037 (0.0121)	0.6444 (0.0112)	0.2685 (0.0187)	0.0343 (0.0018)
	Ensembles	0.8181 (-)	0.6516 (-)	0.8372 (-)	0.0512 (-)

Table 14: Test results on FreeSolv in the format of “metric mean (standard deviation)”.

		RMSE	MAE	NLL	CE
DNN-rdkit	Deterministic	2.2403 (0.1366)	1.6768 (0.1007)	1.3370 (0.1120)	0.0272 (0.0026)
	MC Dropout	2.2316 (0.1070)	1.6469 (0.1122)	1.3357 (0.1257)	0.0247 (0.0015)
	SWAG	2.4516 (0.1188)	1.7853 (0.1478)	1.8461 (0.2920)	0.0358 (0.0043)
	BBP	2.8456 (0.1416)	2.1049 (0.1037)	1.5285 (0.0469)	0.0173 (0.0056)
	SGLD	2.5503 (0.1010)	1.8549 (0.1092)	1.4260 (0.0095)	0.0137 (0.0033)
	Ensembles	1.9627 (-)	1.4359 (-)	1.0149 (-)	0.0240 (-)
ChemBERTa	Deterministic	2.5267 (0.0864)	1.7760 (0.0318)	1.7859 (0.1916)	0.0364 (0.0034)
	MC Dropout	2.5042 (0.0981)	1.7804 (0.0456)	1.7810 (0.1526)	0.0359 (0.0033)
	SWAG	2.6269 (0.1627)	1.8562 (0.1055)	2.2239 (0.2879)	0.0426 (0.0003)
	BBP	2.6340 (0.1368)	1.9072 (0.1600)	1.6143 (0.1930)	0.0322 (0.0066)
	SGLD	2.6564 (0.0357)	1.8633 (0.0344)	1.7627 (0.0809)	0.0347 (0.0053)
	Ensembles	2.3727 (-)	1.6904 (-)	1.5142 (-)	0.0341 (-)
GROVER	Deterministic	2.1352 (0.0193)	1.4770 (0.0303)	2.8244 (0.8307)	0.0428 (0.0034)
	MC Dropout	2.0981 (0.0069)	1.4660 (0.0231)	2.6575 (0.7926)	0.0415 (0.0040)
	SWAG	2.2321 (0.0902)	1.5041 (0.0460)	3.3021 (0.0530)	0.0469 (0.0008)
	BBP	2.6133 (0.0662)	1.8288 (0.0843)	1.4699 (0.0598)	0.0126 (0.0014)
	SGLD	2.1117 (0.0985)	1.3784 (0.0459)	1.2791 (0.1411)	0.0238 (0.0020)
	Ensembles	2.0238 (-)	1.3539 (-)	1.9474 (-)	0.0393 (-)
Uni-Mol	Deterministic	1.7871 (0.1265)	1.2906 (0.0483)	2.5450 (1.2435)	0.0521 (0.0018)
	MC Dropout	1.7585 (0.1322)	1.2652 (0.0559)	2.3425 (1.2327)	0.0515 (0.0018)
	SWAG	1.8524 (0.1449)	1.3481 (0.1063)	2.9865 (1.1583)	0.0545 (0.0013)
	BBP	1.7464 (0.0246)	1.2424 (0.0049)	0.9940 (0.0065)	0.0289 (0.0027)
	SGLD	1.7462 (0.0908)	1.2963 (0.0610)	1.0358 (0.0881)	0.0296 (0.0048)
	Ensembles	1.6716 (-)	1.1780 (-)	1.4306 (-)	0.0504 (-)

Table 15: Test results on Lipophilicity in the format of “metric mean (standard deviation)”.

		RMSE	MAE	NLL	CE
DNN-rdkit	Deterministic	0.7575 (0.0116)	0.5793 (0.0138)	0.6154 (0.2016)	0.0293 (0.0030)
	MC Dropout	0.7559 (0.0110)	0.5773 (0.0132)	0.9071 (0.3721)	0.0341 (0.0052)
	SWAG	0.7572 (0.0101)	0.5823 (0.0129)	0.7191 (0.2267)	0.0308 (0.0027)
	BBP	0.7730 (0.0253)	0.5938 (0.0245)	0.7578 (0.1627)	0.0305 (0.0046)
	SGLD	0.7468 (0.0018)	0.5743 (0.0016)	0.2152 (0.0097)	0.0090 (0.0009)
	Ensembles	0.7172 (-)	0.5490 (-)	0.6165 (-)	0.0322 (-)
ChemBERTa	Deterministic	0.7553 (0.0074)	0.5910 (0.0065)	1.2368 (0.3994)	0.0362 (0.0032)
	MC Dropout	0.7142 (0.0063)	0.5601 (0.0029)	0.8178 (0.2701)	0.0349 (0.0033)
	SWAG	0.7672 (0.0101)	0.5992 (0.0080)	1.5809 (0.4168)	0.0395 (0.0021)
	BBP	0.7542 (0.0050)	0.5869 (0.0087)	0.4419 (0.0775)	0.0279 (0.0023)
	SGLD	0.7622 (0.0045)	0.5982 (0.0070)	0.8719 (0.1359)	0.0355 (0.0020)
	Ensembles	0.7367 (-)	0.5763 (-)	0.9756 (-)	0.0360 (-)
GROVER	Deterministic	0.6316 (0.0066)	0.4747 (0.0040)	2.1512 (0.2203)	0.0478 (0.0009)
	MC Dropout	0.6293 (0.0067)	0.4740 (0.0028)	2.0526 (0.2139)	0.0476 (0.0009)
	SWAG	0.6317 (0.0075)	0.4750 (0.0041)	2.3980 (0.3597)	0.0485 (0.0007)
	BBP	0.6481 (0.0063)	0.5058 (0.0041)	0.0789 (0.0206)	0.0196 (0.0024)
	SGLD	0.6360 (0.0041)	0.4984 (0.0017)	0.0544 (0.0199)	0.0215 (0.0010)
	Ensembles	0.6250 (-)	0.4693 (-)	1.6046 (-)	0.0460 (-)
Uni-Mol	Deterministic	0.6079 (0.0032)	0.4509 (0.0044)	0.8975 (0.5565)	0.0425 (0.0061)
	MC Dropout	0.5983 (0.0099)	0.4438 (0.0117)	1.3663 (1.2187)	0.0440 (0.0084)
	SWAG	0.6026 (0.0004)	0.4476 (0.0022)	1.0101 (0.1639)	0.0453 (0.0012)
	BBP	0.6044 (0.0016)	0.4469 (0.0025)	0.0679 (0.0218)	0.0306 (0.0010)
	SGLD	0.6040 (0.0031)	0.4554 (0.0042)	0.1565 (0.0573)	0.0329 (0.0017)
	Ensembles	0.5809 (-)	0.4266 (-)	0.6450 (-)	0.0438 (-)

Table 16: Test results on QM7 in the format of “metric mean (standard deviation)”.

		RMSE	MAE	NLL	CE
DNN-rdkit	Deterministic	142.9 (2.95)	95.7200 (3.2512)	10.2976 (1.0848)	0.0393 (0.0036)
	MC Dropout	138.7 (2.59)	90.7039 (3.15)	7.4627 (0.4138)	0.0339 (0.0020)
	SWAG	143.7 (1.94)	97.2590 (1.9750)	11.3649 (1.4063)	0.0418 (0.0041)
	BBP	141.5 (4.82)	99.0430 (3.9287)	6.8897 (0.8805)	0.0330 (0.0064)
	SGLD	139.9 (5.48)	99.4873 (2.0159)	5.4071 (0.0338)	0.0098 (0.0019)
	Ensembles	128.7 (-)	84.7269 (-)	5.4568 (-)	0.0281 (-)
ChemBERTa	Deterministic	114.2 (1.95)	66.6504 (3.6637)	6.9619 (1.4000)	0.0251 (0.0059)
	MC Dropout	112.5 (1.20)	64.7828 (3.4349)	6.1942 (0.7998)	0.0309 (0.0061)
	SWAG	114.2 (1.53)	68.0992 (3.5122)	6.9684 (1.3236)	0.0236 (0.0052)
	BBP	116.2 (1.85)	69.9783 (0.3732)	5.5954 (0.2659)	0.0262 (0.0034)
	SGLD	117.0 (0.37)	74.6714 (1.3652)	5.0906 (0.0281)	0.0147 (0.0019)
	Ensembles	111.3 (-)	63.8752 (-)	5.3896 (-)	0.0224 (-)
GROVER	Deterministic	139.6 (3.19)	98.6424 (4.8571)	5.4936 (0.0870)	0.0121 (0.0012)
	MC Dropout	136.2 (2.92)	95.4940 (4.4117)	5.4272 (0.0697)	0.0107 (0.0014)
	SWAG	142.6 (1.32)	107.1310 (1.6574)	5.7041 (0.1256)	0.0153 (0.0018)
	BBP	136.9 (3.20)	99.8460 (2.2180)	5.4555 (0.0135)	0.0035 (0.0007)
	SGLD	159.7 (2.98)	126.6406 (2.8867)	5.5587 (0.0308)	0.0072 (0.0009)
	Ensembles	131.9 (-)	89.4504 (-)	5.3241 (-)	0.0090 (-)
Uni-Mol	Deterministic	103.9 (1.38)	56.6287 (2.3360)	4.6198 (0.2317)	0.0338 (0.0065)
	MC Dropout	103.6 (1.32)	54.8976 (1.3061)	4.5158 (0.2036)	0.0386 (0.0019)
	SWAG	107.8 (0.20)	63.3542 (2.2114)	5.5588 (0.6515)	0.0412 (0.0026)
	BBP	101.5 (1.14)	51.9550 (0.7905)	4.5153 (0.0535)	0.0263 (0.0022)
	SGLD	105.2 (2.63)	57.0601 (4.5219)	4.5642 (0.0453)	0.0290 (0.0014)
	Ensembles	101.2 (-)	52.0409 (-)	4.3732 (-)	0.0360 (-)

Table 17: Test results on QM8 in the format of “metric mean (standard deviation)”.

		RMSE	MAE	NLL	CE
DNN-rdkit	Deterministic	0.0356 (0.0004)	0.0209 (0.0001)	-0.7811 (2.1740)	0.0282 (0.0008)
	MC Dropout	0.0352 (0.0002)	0.0209 (0.0002)	-2.7716 (0.1922)	0.0267 (0.0001)
	SWAG	0.0360 (0.0002)	0.0212 (0.0001)	-0.7143 (1.5808)	0.0289 (0.0005)
	BBP	0.0370 (0.0002)	0.0214 (0.0001)	-0.9807 (0.5485)	0.0269 (0.0004)
	SGLD	0.0446 (0.0008)	0.0294 (0.0005)	-2.7053 (0.0184)	0.0121 (0.0001)
	Ensembles	0.0345 (-)	0.0202 (-)	-3.0118 (-)	0.0279 (-)
ChemBERTa	Deterministic	0.0377 (0.0001)	0.0208 (0.0000)	3.8214 (1.1599)	0.0356 (0.0001)
	MC Dropout	0.0370 (0.0002)	0.0204 (0.0001)	-0.6884 (0.1974)	0.0332 (0.0001)
	SWAG	0.0379 (0.0002)	0.0210 (0.0000)	5.4548 (1.9400)	0.0360 (0.0002)
	BBP	0.0358 (0.0003)	0.0206 (0.0001)	-1.5642 (0.0700)	0.0316 (0.0005)
	SGLD	0.0362 (0.0002)	0.0212 (0.0004)	-3.1380 (0.0611)	0.0169 (0.0007)
	Ensembles	0.0373 (-)	0.0205 (-)	0.9180 (-)	0.0349 (-)
GROVER	Deterministic	0.0319 (0.0007)	0.0174 (0.0003)	0.0201 (1.4388)	0.0386 (0.0020)
	MC Dropout	0.0318 (0.0006)	0.0174 (0.0003)	-0.8810 (1.1057)	0.0381 (0.0021)
	SWAG	0.0323 (0.0004)	0.0176 (0.0003)	0.6655 (0.9582)	0.0409 (0.0013)
	BBP	0.0324 (0.0004)	0.0183 (0.0003)	-3.3037 (0.0260)	0.0199 (0.0005)
	SGLD	0.0340 (0.0007)	0.0205 (0.0007)	-3.1826 (0.0378)	0.0157 (0.0006)
	Ensembles	0.0315 (-)	0.0171 (-)	-1.1036 (-)	0.0383 (-)
Uni-Mol	Deterministic	0.0334 (0.0006)	0.0172 (0.0000)	2.7759 (2.9972)	0.0432 (0.0020)
	MC Dropout	0.0331 (0.0006)	0.0171 (0.0001)	0.8170 (2.8226)	0.0412 (0.0023)
	SWAG	0.0338 (0.0004)	0.0173 (0.0001)	3.5568 (2.5309)	0.0440 (0.0013)
	BBP	0.0309 (0.0007)	0.0164 (0.0002)	-2.4581 (0.4546)	0.0316 (0.0023)
	SGLD	0.0300 (0.0003)	0.0163 (0.0001)	-3.2399 (0.0908)	0.0210 (0.0004)
	Ensembles	0.0331 (-)	0.0169 (-)	-0.0541 (-)	0.0421 (-)

Table 18: Test results on QM9 in the format of “metric mean (standard deviation)”.

		RMSE	MAE	NLL	CE
DNN-rdkit	Deterministic	0.0151 (0.0001)	0.0101 (0.0001)	-3.3798 (0.0592)	0.0442 (0.0003)
	MC Dropout	0.0148 (0.0001)	0.0100 (0.0001)	-3.5269 (0.0258)	0.0433 (0.0003)
	SWAG	0.0152 (0.0002)	0.0102 (0.0001)	-3.2845 (0.0814)	0.0449 (0.0003)
	BBP	0.0153 (0.0002)	0.0103 (0.0001)	-3.3470 (0.0280)	0.0445 (0.0004)
	SGLD	0.0196 (0.0003)	0.0144 (0.0002)	-3.3352 (0.0052)	0.0070 (0.0003)
	Ensembles	0.0143 (-)	0.0096 (-)	-3.6023 (-)	0.0436 (-)
ChemBERTa	Deterministic	0.0146 (0.0004)	0.0092 (0.0002)	-2.4104 (0.0698)	0.0547 (0.0002)
	MC Dropout	0.0141 (0.0002)	0.0088 (0.0001)	-3.1501 (0.1094)	0.0513 (0.0005)
	SWAG	0.0148 (0.0003)	0.0092 (0.0002)	-2.1703 (0.0205)	0.0553 (0.0001)
	BBP	0.0144 (0.0001)	0.0093 (0.0001)	-2.5932 (0.0665)	0.0540 (0.0002)
	SGLD	0.0153 (0.0001)	0.0101 (0.0002)	-3.7586 (0.0106)	0.0338 (0.0007)
	Ensembles	0.0140 (-)	0.0087 (-)	-2.8766 (-)	0.0543 (-)
GROVER	Deterministic	0.0115 (0.0000)	0.0068 (0.0000)	-0.7874 (0.5323)	0.0621 (0.0008)
	MC Dropout	0.0114 (0.0000)	0.0068 (0.0000)	-1.1002 (0.5003)	0.0616 (0.0008)
	SWAG	0.0116 (0.0000)	0.0068 (0.0000)	-0.4778 (0.1923)	0.0625 (0.0002)
	BBP	0.0118 (0.0000)	0.0070 (0.0000)	-1.8855 (0.1189)	0.0591 (0.0004)
	SGLD	0.0136 (0.0006)	0.0088 (0.0003)	-3.7855 (0.0411)	0.0291 (0.0017)
	Ensembles	0.0114 (-)	0.0067 (-)	-1.0286 (-)	0.0620 (-)
Uni-Mol	Deterministic	0.0096 (0.0001)	0.0054 (0.0001)	0.0143 (0.4195)	0.0664 (0.0003)
	MC Dropout	0.0096 (0.0001)	0.0054 (0.0001)	-0.2513 (0.3961)	0.0661 (0.0003)
	SWAG	0.0097 (0.0000)	0.0054 (0.0000)	-0.4624 (0.0619)	0.0660 (0.0001)
	BBP	0.0095 (0.0002)	0.0054 (0.0000)	-2.9595 (0.1250)	0.0618 (0.0003)
	SGLD	0.0095 (0.0001)	0.0055 (0.0001)	-4.2093 (0.0049)	0.0459 (0.0002)
	Ensembles	0.0095 (-)	0.0053 (-)	-0.3192 (-)	0.0663 (-)